

**Genetic relation of CO<sub>2</sub> and its suitable usage in the Peninsular Malay Basin.**

By

Mohd Al Fatah Bin Zakariyah

Final Report submitted in partial fulfillment of  
the requirements for the  
Bachelor of Engineering (Hons)  
Petroleum Engineering

APRIL 2011

Universiti Teknologi PETRONAS  
Bandar Seri Iskandar  
31750 Tronoh  
Perak Darul Ridzuan

CERTIFICATION OF APPROVAL

**Genetic relation of CO<sub>2</sub> and its suitable usage in the Peninsular Malay Basin.**

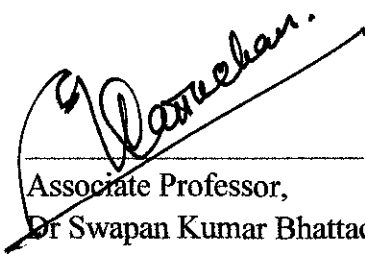
By

Mohd Al Fatah Bin Zakariyah

A project dissertation submitted to the  
Universiti Teknologi PETRONAS  
in partial fulfillment of the requirement for the  
Bachelor of Engineering (Hons)  
Petroleum Engineering

April 2011

Approved by,



Associate Professor,  
Dr Swapan Kumar Bhattacharya,  
Universiti Teknologi PETRONAS,  
Bandar Seri Iskandar ,  
31750 Tronoh,  
Perak Darul Ridzuan

## **CERTIFICATION OF ORIGINALITY**

This is to certify that I am responsible for the work submitted in this project, that the original work is my own except as specified in the references and acknowledgements, and that the original work contained herein have not been undertaken or done by unspecified sources or persons.



---

Mohd Al Fatah Bin Zakariyah

Petroleum Engineering Student  
Universiti Teknologi PETRONAS  
Bandar Seri Iskandar  
31750 Tronoh  
Perak Darul Ridzuan.

## **ACKNOWLEDGEMENT**

First and foremost I would like to express my sincere gratitude to my project supervisor, Associate Professor Dr Swapan Kumar Bhattacharya, for his encouragement, guidance and support from the initial to the final level enabled me to develop an understanding of the subject. I was privileged to experience a sustained enthusiastic and involved interest from his side. This fueled my enthusiasm even further and encouraged me to boldly step into a better student.

My deep sense of gratitude to PETRONAS Carigali Sdn Bhd and PETRONAS Management Unit for provides me the data to complete this project. Thanks and appreciation to the helpful people at PETRONAS Carigali Sdn Bhd and PETRONAS Management Unit, for their support.

Last but not least, I would also thank to Universiti Teknologi PETRONAS and Faculty of Geosciences and Petroleum Engineering without whom this project would have been a distant reality. I also extend my heartfelt thanks to my family and fellow clique.

## ABSTRACT

Reservoirs with high CO<sub>2</sub> content are common throughout the Asia Pacific region, notably the Gulf of Thailand, Malaysia, Indonesia and Vietnam. In Malay Basin, CO<sub>2</sub> production ranges from 5 to 90% mol. The high production of CO<sub>2</sub> is concentrated in certain region in the Malay Basin. The most notable high production of CO<sub>2</sub> is the northern region near Thailand and the center of Malay Basin. The comprehensive study on CO<sub>2</sub> genetic relation and its source haven't been established yet. For this project the authors have studied the origin of produced CO<sub>2</sub> in order predicts the continuous supply for field development program. The author also made a comprehensive study on the tectonic framework, stratigraphy, various plays and geothermal gradient of Malay Basin to relate with the existence of associated gas. For the development program EOR operation is preferable among others since it is the suitable due to numerous of CO<sub>2</sub> supply from the field. The CO<sub>2</sub> flooding operation will be discussed in this report where the details modeling for reservoir and well are established to predict the performance of the reservoir with CO<sub>2</sub> flooding. Results from the modeling indicate CO<sub>2</sub> flooding as EOR may be suitable for further development plan to increase the production of oil up to 20 % from naturally flow well. In the final chapter of this report, the author relates the stratigraphy, heat flow and plays in Malay Basin to conclude the finding on origin of CO<sub>2</sub> in Malay Basin. The high production of CO<sub>2</sub> is mainly originated from inorganic origin while low production of CO<sub>2</sub> is from organic origin. The isotopic value of  $\delta^{13}\text{C}$  is used to distinguish between these two types of CO<sub>2</sub>.

## **Contents**

<b>PROJECT BACKGROUND</b> .....	5
1.1 Background study .....	5
1.2 Problem Statement.....	5
1.3 Objective.....	7
1.4 Scope of Study .....	7
1.5 The relevancy of the project .....	7
<b>LITERATURE REVIEW</b> .....	8
2.1 Sources of Carbon Dioxide.....	8
2.1.1 Thermal degradation of organic matter.....	8
2.1.2 Thermal breakdown of carbonates.....	8
2.1.3 Inorganic clay reaction.....	8
2.2 Isotopes of carbon.....	9
2.2.1 Stable Isotopes .....	9
2.3 Malay Basin (The Petroleum Geology and Resources of Malaysia, 1999).....	11
2.3.1 Tectonic Framework.....	11
2.3.2 Stratigraphy and Palaeoenvironments .....	13
2.3.3 Hydrocarbon Plays and Trap styles .....	15
2.3.4 Migration and Entrapment.....	16
2.4 Prediction of CO <sub>2</sub> occurrence in South East Asia (Scott W. Imbus L*, B. J. (1998)).....	17
2.4.1 Empirical associations with basin attributes .....	18
2.4.2 Statistical associations with reservoir attributes and fluid composition .....	18
2.4.3 Neural network analysis.....	19
2.5 Organic-rich tropical rivers and their role in CO <sub>2</sub> and methane generation (Robert C Shoup, and Yutthorn Gonnecome, 2009) .....	20
2.5.1 Origin Theory .....	21
2.6 Carbon isotopic signature of CO <sub>2</sub> in Arthit gas field, Northern Malay basin, the Gulf of Thailand (S. Pisutha-Arnond & A. Sirimongkolkitti, V. Pisutha-Arnond , 2008 ).....	22

2.7 Possible Inorganic Origin of the High CO <sub>2</sub> Gas Reservoirs in the Platong and the Erawan Gas Fields, Gulf of Thailand (Masashi Fujiwara, Makoto Yamada, Akio Sasaki, 2009) .....	27
2.8 Enhanced Oil Recovery in Malaysia: Making it Reality (M.K Hamdan, N. Darman, D. Hussain, Z. Ibrahim) .....	28
2.8.1 Challenges and Obstacles .....	29
2.9 Enhanced Oil Recovery in Malaysia: Making it Reality Part 2 (Y. Samsudin, N. Darman, D. Husain, M.K Hamdan, PETRONAS Carigali Sdn Bhd, 2005).....	30
2.9.1 Dulang Field (Immiscible WAG) .....	30
2.9.3 West Lutong Field.....	31
3.0 Petex (Petroleum Experts) .....	31
3.0.1Mbal.....	31
3.0.2 PROSPER.....	32
3.1 Material Balance Principle.....	33
3.1.1 Gas Cap Expansion .....	34
3.1.2 Release gas volume.....	35
3.1.3 Remaining Oil Volume .....	35
3.1.4 Rock and Connate Water Expansion .....	35
3.1.5 Water Influx.....	36
<b>METHODOLOGY</b> .....	<b>37</b>
3.1 Methodology Flowchart.....	37
3.3 Distribution of CO <sub>2</sub> in Malay Basin.....	38
3.4 CO <sub>2</sub> flooding modeling .....	39
3.4.1 Reservoir modeling.....	40
Data preparation.....	40
Reservoir definition .....	41
PVT correlations matching .....	41
3.4.2 Well modeling.....	41
PVT correlation matching.....	42
IPR prediction .....	42
Vertical Flow Correlation Matching.....	42

Injector Well .....	43
<b>RESULTS AND DISCUSSION</b> .....	<b>44</b>
4.1 CO <sub>2</sub> genetic relation .....	44
4.2 Results from modeling .....	45
<b>CONCLUSION</b> .....	<b>48</b>
<b>REFERENCES</b> .....	<b>50</b>
Gantt chart for FYP 1 .....	51
Gantt chart for FYP 2 .....	52
Project Activities for FYP 1 .....	53
Project activities for FYP 2 .....	53

## List of Figures

Figure 1: Malay Basin (Petroleum System of Malay Basin Province Malaysia, 2002).....	6
Figure 2 : Gas Reserves in Malaysia.....	6
Figure 4 : Antclines Axes zones (The Petroleum Geology and Resources of Malaysia, 1999) ..	12
Figure 3: Basement Depth and faults zones (The Petroleum Geology and Resources of Malaysia, 1999).....	12
Figure 5: Structural and Fault zones (The Petroleum Geology and Resources of Malaysia, 1999) .....	12
Figure 6: Generalised stratigraphy, hydrocarbon occurrences and structural history of the Malay Basin (EPIC, 1994).....	13
Figure 7: Cross section of Malay Basin with different trapping style zones (The Petroleum Geology and Resources of Malaysia, 1999) .....	15
Figure 8: Cross section of Malay Basin with different trapping style zones (Resource: The Petroleum Geology and Resources of Malaysia, 1999).....	16
Figure 9: Heat Flow in the Malay Basin zones (Resource: The Petroleum Geology and Resources of Malaysia, 1999).....	16
Figure 10: Geothermal gradient in the Malay Basin zones (Resource: The Petroleum Geology and Resources of Malaysia, 1999).....	17
Figure 12: Carbon isotope fractionation factors of CO <sub>2</sub> and.....	24
Figure 13: Cross plot between CO <sub>2</sub> contents and carbon.....	25
Figure 14: Carbon isotope compositions of major carbon.....	25
Figure 15: Cross plot between CO <sub>2</sub> contents and Carbon isotopic .....	26
Figure 16: The generation of gases from organic matter with.....	26
Figure 11: Oil reserves in Malaysia .....	28
Figure 17: Mbal workflow .....	32
Figure 18 : Material Balance Principle .....	34
Figure 19 : Distribution of CO <sub>2</sub> in the Malay Basin (The Petroleum Geology and Resources of Malaysia, 1999) .....	38
Figure 20 : Contour map of CO <sub>2</sub> distribution (The Petroleum Geology and Resources of Malaysia, 1999) .....	38
Figure 21: Cross plot of Cross plot of $\delta^{13}C$ against mole % for CO <sub>2</sub> in Malay Basin (The Petroleum Geology and Resources of Malaysia, 1999).....	44
Figure 22 : CO <sub>2</sub> migration route (The Petroleum Geology and Resources of Malaysia, 1999) ..	45
Figure 23: Reservoir production (without CO <sub>2</sub> flooding).....	45
Figure 24: Reservoir production (with CO <sub>2</sub> flooding) .....	46

# CHAPTER 1

## PROJECT BACKGROUND

### 1.1 Background study

The Malay Basin, located to the south of the Gulf of Thailand, covers an area of around 80,000 km<sup>2</sup> with sediment thickness up to 14 km in the basin centre. The basin can be broadly subdivided into a northern-central gas-prone province and a southern oil-prone province, save for some minor exceptions to this generalization such as the gas trend occurring in the south western margin and the oil trend on the north eastern flank of the basin. The abundance of hydrocarbon reserves testifies to the presence of effective Oligocene/Early Miocene and Early Miocene/Middle Miocene petroleum systems, each sourced by lacustrine and fluviodeltaic source rocks, respectively. Both hydrocarbon and non-hydrocarbon (particularly carbon dioxide) gases also occur as large accumulations in the Malay Basin. Furthermore, the accumulation of carbon dioxide is reported higher in the north of Malay Basin. As such carbon dioxide prediction is an important aspect for future exploration and also for commercialized purposes.

### 1.2 Problem Statement

The amount of CO<sub>2</sub> encountered in wells in the Malay Basin (Figure 1) varies from a few percentage points to as high as 90%. Although the geographical distribution of CO<sub>2</sub> in the Malay Basin is probably understood, the stratigraphic distribution of CO<sub>2</sub> still poses many questions. So far, there is no predictive technique available to estimate the genetic relation and concentrations of CO<sub>2</sub> production in Malay Basin. It is important to understand the source and the distribution of the CO<sub>2</sub> and how it can be fully utilize to increase the production of declining field nearby.

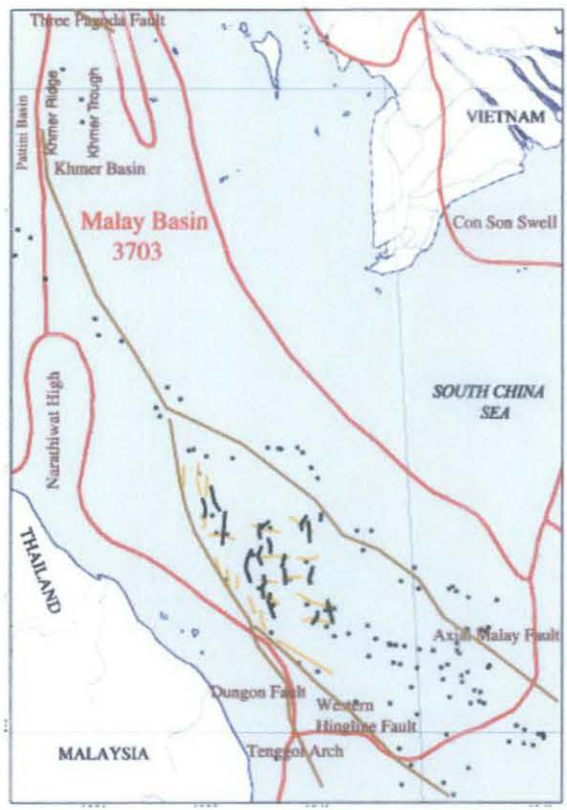


Figure 1: Malay Basin (Petroleum System of Malay Basin Province Malaysia,

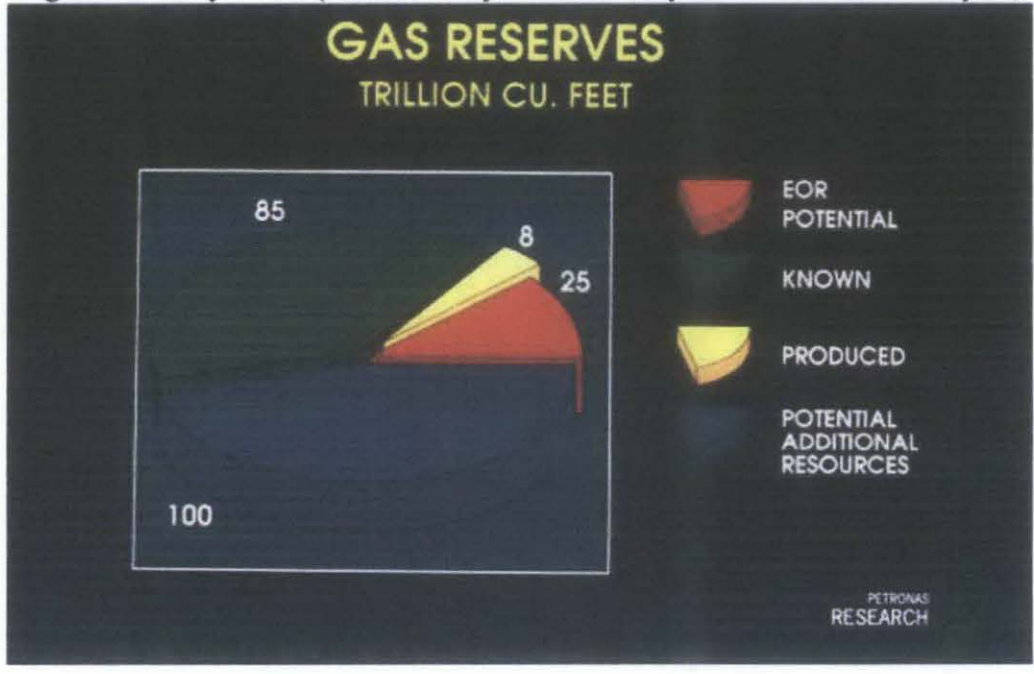


Figure 2 : Gas Reserves in Malaysia

### **1.3 Objective**

The main objectives of this project are to study the genesis of carbon dioxide in the Malay Basin to understand its magnitude as supply source. The geologic information and geothermal gradient of Peninsular Malay Basin will be studied to determine the relation between genesis of carbon dioxide with thermal changes. The second objective is to study the modes of commercial utilization of produced carbon dioxide. In this context, the author will focus on CO<sub>2</sub> flooding.

### **1.4 Scope of Study**

Production of carbon dioxide in the Malay Basin

Reservoir Engineering

Reservoir rock and properties

Petroleum Geosciences

Reservoir Rock and Fluid Properties

Petroleum Experts (PROSPER, MBAL)

In the nutshell, students need to apply their knowledge gained in study into real solving problems situation.

### **1.5 The relevancy of the project**

This project allows students to:

- Integrate and relate the knowledge acquired from the various petroleum engineering sub-disciplines.
- This project is relevant for EOR study for PETRONAS.

## CHAPTER 2

### LITERATURE REVIEW

#### 2.1 Sources of Carbon Dioxide

There are four sources which carbon dioxide CO<sub>2</sub> can be produced, one organic and three inorganic.

##### 2.1.1 Thermal degradation of organic matter

In organic process, the carbon dioxide is produced resulted from thermal degradation of organic matter which occurs during diagenesis and catagenesis. Both of this process plays important role in hydrocarbon generation. Diagenesis is a changes and alterations that take place on skeletal (biological) material in a burial context that done by bacterial activity and low-temperature chemical reactions. It covers temperature range up to approximately 50°C. Chain decomposition activity form kerogen to condensate and gas with increasing temperature is called catagenesis. The catagenesis range is from about 50°C to 200°C.

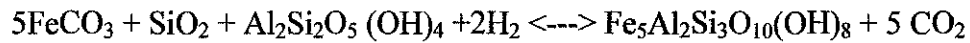
##### 2.1.2 Thermal breakdown of carbonates

Carbon dioxide from this reaction is a result of endothermic reaction of thermal cracking of carbonates at high temperature probably. Group 2 of carbonates decomposed on heating to produce carbon dioxide as explained by below reaction



##### 2.1.3 Inorganic clay reaction

The inorganic source is important source of CO<sub>2</sub> in the deeper sections of sedimentary basin (Hutcheon et al, 1980). The reaction is explains by following expression.



The isotopic composition of this  $\text{CO}_2$  depends on the isotopic composition of the precursor carbonate. However the average isotopic composition of carbonates in metamorphic rock is around -6% (Ohmoto and Rye, 1979).

#### **2.1.4 Volcanic Activity**

Carbon dioxide can be derived from several sources in volcanic area which are subduction and or partial melting or the metamorphism of the siliceous or carbonate rock/sediments (Mary et. Al 2001). Arc volcanic gases can also incorporate carbonate rich fluids from crustal metamorphism and metasomatic reaction triggered by magmatic heating. The third source of carbon dioxide is volatilization of entrapped water itself at mean temperature and pressure (J.P Lockwood, Richard W Hazlet, 2010).

### **2.2 Isotopes of carbon**

Isotopes are different types of atoms (nuclides) of the same chemical element, each having a different number of neutrons. In a corresponding manner, isotopes differ in mass number (or number of nucleons) but never in number. The number of protons (the atomic number) is the same because that is what characterizes a chemical element. For example, carbon-12, carbon-13 and carbon-14 are three isotopes of the element carbon with mass numbers 12, 13 and 14, respectively. The atomic number of carbon is 6, so the neutron numbers in these isotopes of carbon are therefore  $12-6 = 6$ ,  $13-6 = 7$ , and  $14-6 = 8$ , respectively.

#### **2.2.1 Stable Isotopes**

The isotopes for  $\text{C}^{12}$  and  $\text{C}^{13}$  are stable isotopes. The isotope  $\text{C}^{13}$  is distributed sediments of all geological ages and can be used to solve many geochemical problems because its difference in mass relative to carbon-12 results in fractionation by both biological and physical processes.

$$\delta^{13}\text{C} = \left( \frac{\left(\frac{^{13}\text{C}}{^{12}\text{C}}\right)_{\text{sample}}}{\left(\frac{^{13}\text{C}}{^{12}\text{C}}\right)_{\text{standard}}} - 1 \right) \times 1000 \text{ ‰}$$

Above equation calculate the ratio difference of C<sup>13</sup> per C<sup>12</sup> in parts per thousand, relative to the standard. The standard established for C<sup>13</sup> work was the Pee Dee Belemnite or (PDB) and was based on a Cretaceous marine fossil, Belemnitella Americana, which was from the Pee Dee Formation in South Carolina. This material had an anomalously high <sup>13</sup>C: <sup>12</sup>C ratio and was established as <sup>13</sup>C value of zero. Use of this standard gives most natural material a negative δ<sup>13</sup>C (<http://en.wikipedia.org/wiki/%CE%9413C>).

Source	δ <sup>13</sup> C‰
Thermal degradation of organic matter	-8 to -12
Thermal destruction of carbonates	+4 to -5
Bacterial oxidation of methane	-20 to -59
Volcanic degassing	-8
Atmospheric CO <sub>2</sub>	-8

Table 1 : Variation in δ<sup>13</sup>C of CO<sub>2</sub> from Different Sources

Above table explains that different sources of carbon dioxide cause different δ<sup>13</sup>C values of carbon. As we can see thermogenic CO<sub>2</sub> from organic material has more negative δ<sup>13</sup>C values from decomposition of carbonates while bacterial oxidation of methane results in wide range of δ<sup>13</sup>C value.

## **2.3 Malay Basin (The Petroleum Geology and Resources of Malaysia, 1999)**

The Malay Basin is situated in the southern part of the Gulf Of Thailand between Vietnam and Peninsular Malaysia. The basin continues northwestwards to merge with Thailand's Pattani Trough and southwestwards with the Indonesia's West Natuna Basin (Figure Below).

### **2.3.1 Tectonic Framework**

The Malay Basin is located at the center of Sundaland, the cratonic core of Southeast Asia and elongate NW-SE trending, about 500 km long and 250 km wide underlain by a pre-Tertiary basement of metamorphic, igneous and sedimentary rocks. The basin is bounded by relatively shallow basement; the Terengganu Platform and Tenggol Arch to the southwest, the Narathiwat High to the northwest. The basement represents the late Mesozoic continental landmass that existed before the basins were formed. The Malay Basin is asymmetrical along its length and in cross section. Its southwestern flank is slightly steeper than its northeastern flank. Basement faults in the southeastern and central parts of the basin mostly trend E-W represent overall basin trend. The southwestern margin is marked by the Western Hinge Fault (WHF). To the south of WHF the Tenggol Fault marks the northeastern edge of Tenggol Arch. The Dungun Fault is a splay of the WHF that cut across the Terengganu platform on the southwestern flank of the Malay Basin. The Malay Basin is a complex rift composed of numerous extensional grabens. Most of these grabens have been penetrated because of their great depths but were interpreted from magnetic, gravity, and seismic data (Mazlan B Hj Madon, Peter Abolins, Mohammad Jamal B Hoesni, Mansor B. Ahmad, 1999).

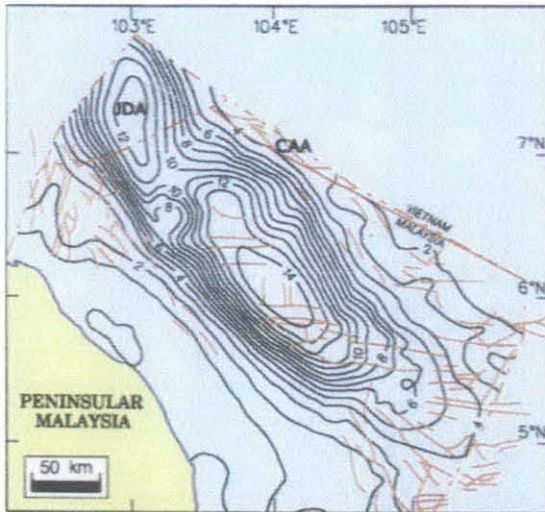


Figure 4: Basement Depth and faults zones (The Petroleum Geology and Resources of Malaysia, 1999)

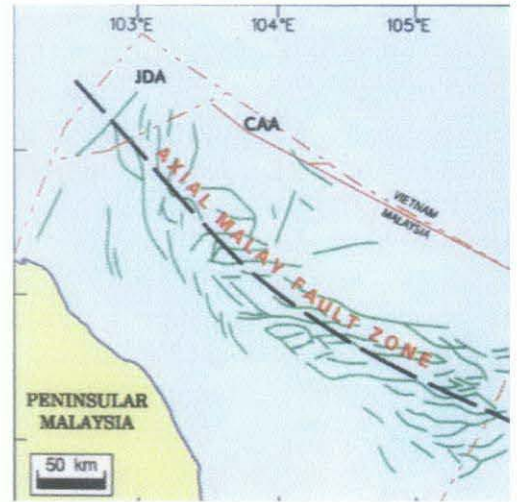


Figure 3 : Anticlines Axes zones (The Petroleum Geology and Resources of Malaysia, 1999)

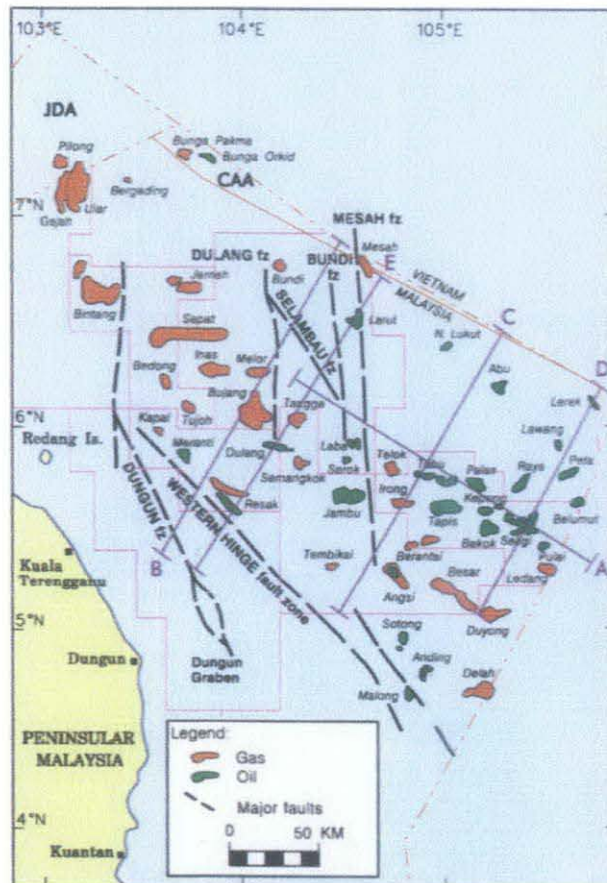


Figure 5: Structural and Fault zones (The Petroleum Geology and Resources of Malaysia, 1999)

### 2.3.2 Stratigraphy and Palaeoenvironments

The Malay Basin strata are subdivided into seismic stratigraphic units. Each unit is bounded by basin-wide seismic reflectors. The groups are designated alphabetically in order of increasing age, from A to M. The stratigraphic development of the Malay Basin is directly related to its structural evolution which occurred in 3 phases: 1) a pre Miocene (Oligocene or earlier) extensional or synrift phase, 2. An Early to Middle Miocene thermal/tectonic subsidence phase and 3. a late Miocene –Quaternary subsidence phase.

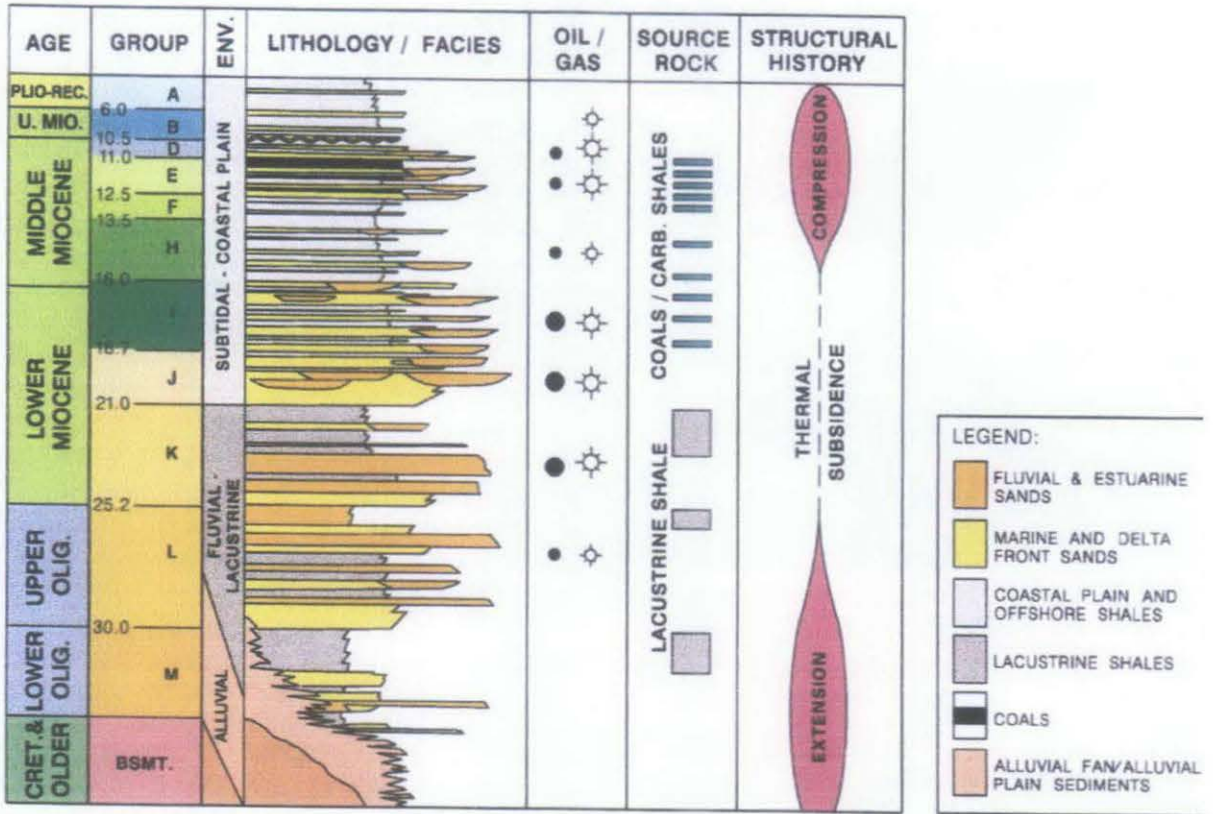


Figure 6: Generalised stratigraphy, hydrocarbon occurrences and structural history of the Malay Basin (EPIC, 1994)

The pre-Miocene phase represents the extensional phase of the basin development, during which subsidence was controlled by faulting. Initially, sedimentation in isolated

half graben depocenters deposited thick synrift successions of alternating sand-dominated and shale-dominated, fluviolacustrine sequences (figure above). Group M to K, which fill the extensional sub-basins, comprise the deposits of braided streams, coastal plains, lacustrine deltas and lakes. These deposits show increasing lacustrine influence towards the basin center (Mohd Tahir Ismail et al., 1994). Extensional faulting ceased during Late Oligocene. Continued thermal subsidence, however resulted in deposition of Group L to D. The basin was probably at or near sea level by Early Miocene times, as indicated by the abundance of coal-bearing strata in the succession. The first sign of the marine inundation were recognized from micropalaeontology within Lower Miocene strata (Azmi Mohd Yazkzn et al., 1994; Mohd Tahir Ismail et al., 1994). A cyclic succession of offshore marine, tidal-eustrine, coastal plain and fluvial sediments was deposited in the Lower to Middle Miocene. Groups I and J consist of progradational to aggradational fluvial to tidally-dominated estuarine sands. Group H and F are dominantly marine to deltaic sediments with fluvial/eustrine channels, deposited during an overall sea-level rise. Group E and D were deposited by the progradational stacking of dominantly fluvial/estuarine channels and culminated with a localized erosional unconformity. The Early-Middle Miocene period of thermal/tectonic subsidence was accompanied by compressional deformation which resulted in local inversion of half grabens by re-activation of their bounding faults and a major uplift in the southeastern part of the basin. The unconformity is overlain by undeformed marine sediment of Groups A and B. Deformation was contemporaneous with sedimentation, such that erosion and non-deposition on the crests of the structures occurred simultaneously with deposition on the flanks. It is estimated that up to 1200m of sediment may have eroded off the crests of some structures (Murphy 1989). Inversion is more severe in the southeastern part of the basin; while sedimentation of Groups D, E and F in the central and northern parts of the basin was relatively continuous. Sediments in the north may have been derived partly from erosion of pre-existing sediment in the south.

### 2.3.3 Hydrocarbon Plays and Trap styles

#### Compression Anticlines

Hydrocarbon distribution map indicates that compressional anticlines in south are oil-prone while those in the northern part are gas prone. In the south, most of anticlines are either domal or asymmetrical and often compartmentalized by normal faults. The main reservoirs are shallow marine and fluvial sandstones of Group H, I, J and K. The compressional anticlines in the central part of the basin involves reservoir in Group D and E sands. Most traps are formed by 4-way dip closures in domal structures or asymmetrical anticlines and normal fault-bounded structures as shown in Figure 5 and 6. The reservoirs are formed by shallow marine sandstone of Group D and E. There are major gas trend in the southwestern part of the basin, close to the Tenggol Fault. This is the Angsi-Duyong trend (Figure 6). These larger compressional anticlines are structurally similar to those in the main oil province to the north, and are underlain by synrift half-grabens controlled by normal faults.

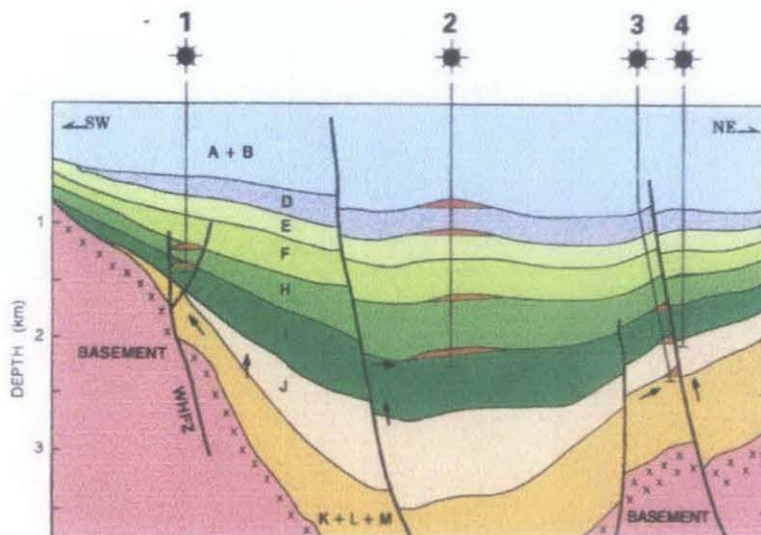


Figure 7: Cross section of Malay Basin with different trapping style zones (The Petroleum Geology and Resources of Malaysia, 1999)

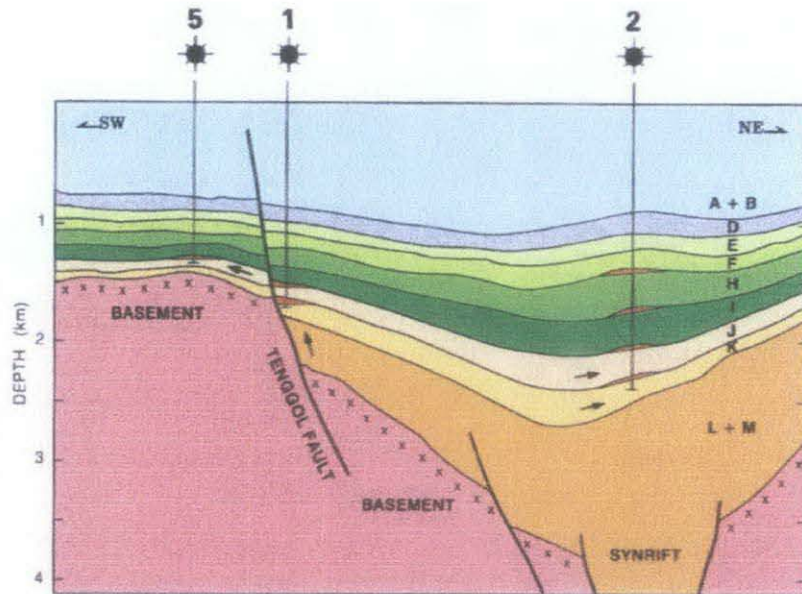


Figure 8: Cross section of Malay Basin with different trapping style zones (Resource: The Petroleum Geology and Resources of Malaysia, 1999)

### 2.3.4 Migration and Entrapment

The Malay Basin is a relatively young Tertiary basin which explains the significantly high present-day surface heat flow especially northern and central parts of the basin. Geothermal in Malay Basin vary from about  $32^{\circ}\text{Ckm}^{-1}$  on the flank and increase to  $53^{\circ}\text{Ckm}^{-1}$  in the basin centre basin (Figure 8). High Heat flows of around  $105\text{mWm}^{-2}$  are recorded in the axial region, decreasing towards the basin flanks (Figure 7).

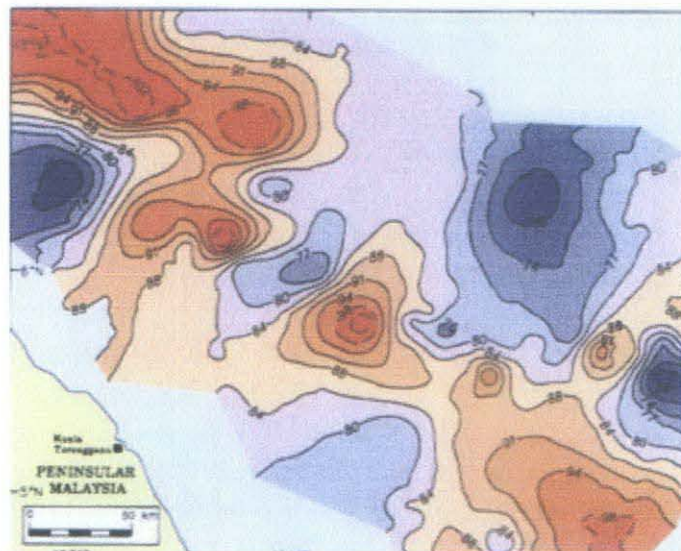


Figure 9: Heat Flow in the Malay Basin zones (Resource: The Petroleum Geology and Resources of Malaysia, 1999)

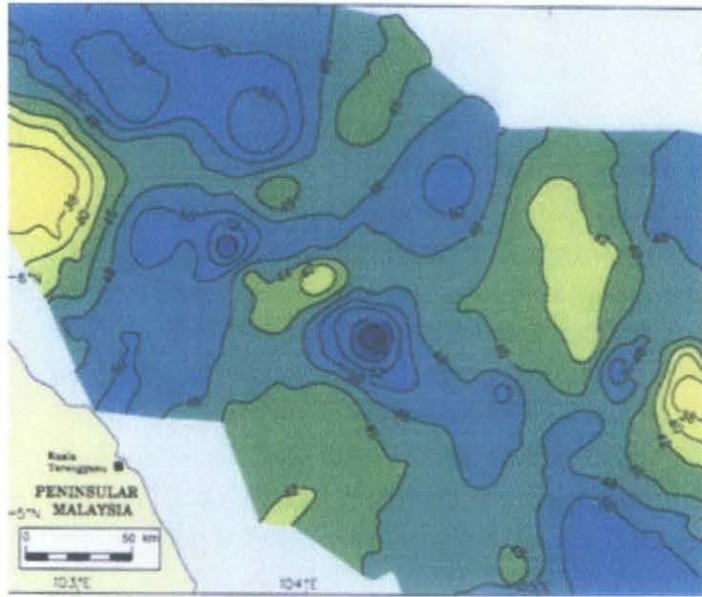


Figure 10: Geothermal gradient in the Malay Basin zones (Resource: The Petroleum Geology and Resources of Malaysia, 1999)

#### 2.4 Prediction of CO<sub>2</sub> occurrence in South East Asia (Scott W. Imbus L\*, B. J. (1998))

In this study a detailed basin model and geohistories and available comprehensive compositional and isotopic data on hydrocarbon/ non-hydrocarbon gas component are constructed. All of the data are examined at four different levels of details.

- (1) Circumstantial- assigning origin based on the presence or absence of major known or suspected geologic elements.
- (2) Empirical- tally of CO<sub>2</sub> level vs. geologic elements over the entire study area.
- (3) Statistical - cross plotting and linear regression of % CO<sub>2</sub> and numerical reservoir attribute and fluid data for a set of basin complexes (two or more basins of similar tectonic setting and in geographic proximity).
- (4) Neural network - multivariate analysis of pre-screened, potentially influential parameters over the entire study area.

## **Results**

### **Circumstantial- assigning origin based on the presence or absence of major known or suspected geologic elements**

Geological features (for example: basement type, sediment thickness) and high geothermal gradient have no effect in the production of CO<sub>2</sub>.

Table 2: Possible influences on CO<sub>2</sub> distribution

#### **2.4.1 Empirical associations with basin attributes**

CO<sub>2</sub> abundance is categorized as (low= <10%, moderate =10-25%, high= >25%). Basin related influences in Table 2 are termed the empirical approach. Among the associations made are seen in Table 3. Basinal factors such as specific tectonic setting and major structural features (e.g. fault type and density) have a significant effect on CO<sub>2</sub> abundance while major basinal factor (such as thermal alteration of carbonates and humic organic matter) doesn't affect the CO<sub>2</sub> production.

#### **2.4.2 Statistical associations with reservoir attributes and fluid composition**

Reservoir-related attributes are considered qualitatively (e.g. % CO<sub>2</sub> vs lithology) and quantitatively (%CO<sub>2</sub> vs depth, pressure, temperature, porosity, permeability, water saturation, % N<sub>2</sub> and % H<sub>2</sub>S content and % gas dryness. The raw data used are compiled in Table 4. Carbon dioxide levels appear to be slightly higher in carbonate, relative to clastic reservoirs (mean: 18.4 vs 11.3%, respectively). Mixed clastic and carbonate reservoirs appear to have the lowest CO<sub>2</sub> levels (mean: 7.4%). Cross-correlations (linear regression) between % CO<sub>2</sub> and numerical parameters yield a significant correlation only for reservoir temperature as shown in Figure. 3. Reservoir-related attributes, compiled with respect to basin complexes (two or more basins of similar tectonic setting and geographic proximity) were used in an effort to detect

specific associations with CO<sub>2</sub> abundance. In this study, reservoir-related attributes, compiled over five basin complexes, are observed to have the following statistically significant correlations with CO<sub>2</sub> level. The basins are: 1) Brunei-Sabah/Sarawak/Sokang, 2) Java (East and West)/ Sunda, 3) Mahakam/Tarakan, 4) Malaya/ Natuna /Thai and 5) Sumatra (Central, North, South).

In Java (East and West)/ Sunda it is shown that CO<sub>2</sub> content increase with depth, under ordinary circumstances, should be accompanied by similar increases in CO<sub>2</sub> content with temperature and pressure. Increases in CO<sub>2</sub> content with depth (and temperature/pressure) could represent basinal or reservoir processes. Correlations with reservoir lithology, porosity, permeability and H<sub>2</sub>S likely represent reservoir-related processes (e.g. diagenesis). Strong positive correlations between CO<sub>2</sub> content and depth and temperature also suggest the prevalence of reservoir related processes on % CO<sub>2</sub> in the Sumatra (Central, North and South) basin complex. Furthermore, the strong positive correlation between CO<sub>2</sub> and H<sub>2</sub>S in this basin complex suggests the involvement of thermo chemical sulfate reduction in CO<sub>2</sub> generation (the amount and distribution of the data, however, are very limited). Secondary processes (see Table 2) responsible for CO<sub>2</sub> enrichment are more difficult to infer than basin- or reservoir-related processes. More detailed data and an understanding of these processes will require basin modeling. This is particularly true for documenting the influence of CO<sub>2</sub> vs hydrocarbon content from processes such as phase segregation (PVT behavior) and differential solubility that occur during migration from source to reservoir or during remigration.

#### **2.4.3 Neural network analysis**

The neural network approach to inferring the origin and occurrence of CO<sub>2</sub> in Southeast Asia incorporates basin features, reservoir attributes and fluid composition. The neural network analysis ranks the relative influence of ten parameters (found to have potential influence during

pre-screening by non-linear regression) as follows: reservoir pressure ~ basin type (Klemme) > basement fault density > reservoir lithology > reservoir permeability ~ reservoir temperature > reservoir water saturation > basin length/width aspect ratio > basin size. The collective correlation coefficient ( $r^2$ ) for 103 observations is 0.59 ( $r = 0.76$ ) and data scatter between predicted and observed CO<sub>2</sub> is sufficiently constrained to be useful in roughly predicting of CO<sub>2</sub> content. The importance of reservoir pressure (apparently related to overpressure situations as reservoir depth and temperature do not appear highly influential) may reflect the increased solubility of CO<sub>2</sub> with pressure or the composition of fluids prior to reservoir breaching. The high rankings of basement fault density (also found by the empirical assessment to be influential) and basin tectonic setting (Klemme's basin classification) attest to the association between CO<sub>2</sub> abundance and young, tectonically active basins with migration conduits for volcanic and metamorphic fluids. It is expected that a neural network study of individual basin complexes or basins (with more complete data) would improve the predictive capability of this technique.

## **2.5 Organic-rich tropical rivers and their role in CO<sub>2</sub> and methane generation (Robert C Shoup, and Yutthorn Gonnecome, 2009)**

Reservoirs contains high CO<sub>2</sub> productions are common throughout the Asia Pacific region, notably the Gulf of Thailand, Malaysia, Indonesia and Vietnam. There are two main possibilities which this CO<sub>2</sub> originated which either by thermogenic alteration of basement or carbonates or diagenetic breakdown of organic material in shallow depth.

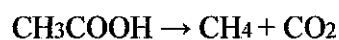
In north Malay Basin, there are 3 trends production of CO<sub>2</sub> with relative to depth. The first trend shoes that the percentage of CO<sub>2</sub> increase gradually with depth from 0% to approximately 30% or less CO<sub>2</sub> production. The second trend explains the increment in CO<sub>2</sub> production from 0% to 80%, before decreasing back to 10% to 30% with increasing depth. The third depth versus CO<sub>2</sub> percentage trend observed in the North Malay Basin is characterized by a relatively rapid increase in the percentage of CO<sub>2</sub> from 0% to approximately 80% or higher. No break back to lower CO<sub>2</sub> percentages are observed in this

CO<sub>2</sub> trend, however, the maximum CO<sub>2</sub> values are encountered near the well total depth. It is conceivable that had these wells drilled deeper, a reduction of CO<sub>2</sub> percent may have occurred.

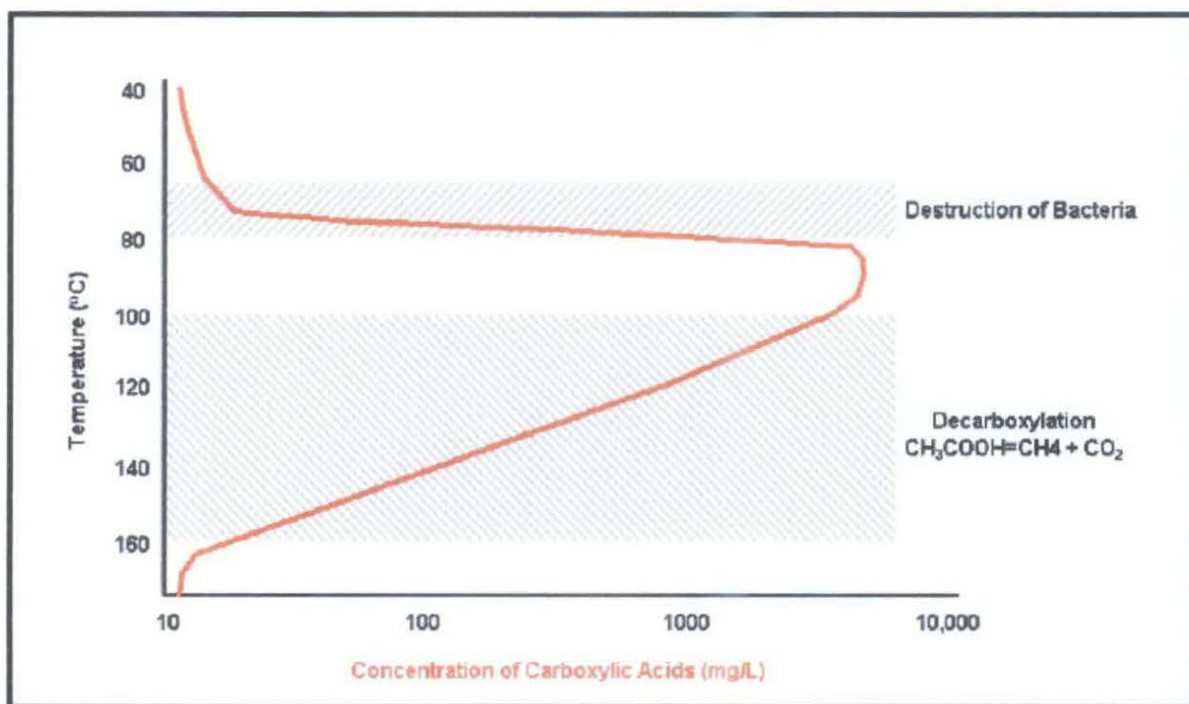
### 2.5.1 Origin Theory

The most relevant theory of inorganic CO<sub>2</sub> is from thermal breakdown of carbonates probably in basement. However results obtain from well cutting shoes that North Malay Basin is underlain by granitic basement and not carbonates as predicted earlier. Therefore it is unlikely that the carbonates are the source. The second possible explanation for the inorganic CO<sub>2</sub> encountered in the North Malay Basin is that it is sourced from the mantle. It is possible that mantle-generated CO<sub>2</sub> migrates into the shallow section along deep-seated faults. If mantle-derived CO<sub>2</sub> is the source of CO<sub>2</sub> in the North Malay basin, it would be expected that the percent of CO<sub>2</sub> would increase with depth as observed in trend 3. However, the decrease of CO<sub>2</sub> percent with depth as seen in trend 2 is not readily explained by migration of mantle-derived CO<sub>2</sub>, or any deep-sourced CO<sub>2</sub>.

The most likely source for CO<sub>2</sub> in the North of Malay Basin is from the degeneration of organic compound during diagenesis and catagenesis process. In the first stage of diagenetic process, bacterial decomposition of interbedded organic material will result in the generation of carboxylic acid anions. At reservoir temperatures between 80° and 120° C the concentrations of carboxylic acid anions will increase exponentially. As formation temperatures increase with increased burial, the carboxylic acid anions are destroyed by thermal decarboxylation. Although destruction of carboxylic anions will initiate at approximately 100° C, the maximum rate of carboxylic anion destruction occurs between 120° and 200° C (Figure 3). During the process of thermal decarboxylation, both methane and CO<sub>2</sub> are generated by following equation



The process of CO<sub>2</sub> generation by diagenesis seems to provide the best explanation for the distribution of CO<sub>2</sub> observed in the North Malay Basin. The highest concentration of CO<sub>2</sub> in the North Malay Basin occurs in the northernmost portion of the basin in the region of the Kim Quy High. The present-day reservoir temperatures across the Kim Quy High range from 100°C and 140°C which are ideal for the generation of CO<sub>2</sub> through thermal decarboxylation.



## 2.6 Carbon isotopic signature of CO<sub>2</sub> in Arthit gas field, Northern Malay basin, the Gulf of Thailand (S. Pisutha-Arnond & A. Sirimongkolkitti, V. Pisutha-Arnond , 2008 )

Arthit gas field located at northwestern margin of the Malay Basin with area approximately 3900 km<sup>2</sup>. Carbon dioxide production discovered in this field ranging from less than 10% to as high as 90%. The objective of this study is to discuss the distribution of carbon isotopic data of CO<sub>2</sub> and its contents. 60 samples are obtained from RFT and TST from 19 wells drilled during 1999 to 2002 and this sample will be

evaluated to study the sources and migration of CO<sub>2</sub> in Arthit gas field. Figure 2 shows the carbon isotopic fractionation factors between CO<sub>2</sub> and CH<sub>4</sub>. The triangle symbols are the equilibrium carbon isotopic fractionation curve given by Friedman and O'Neil (1977). The grey circles (packed into grey line) are the equilibrium carbon isotopic fractionation line proposed by Horita (2001; cited in Chacko et al., 2001). The fractionation factor given by Hotari (2001) is in good agreement with that of Friedman and O'Neil (1977). The  $\Delta(\delta^{13}\text{C CO}_2 - \delta^{13}\text{C CH}_4)$  are plotted against the formation temperatures from Arthit gas field in Figure 12 in order to test whether the CO<sub>2</sub> and CH<sub>4</sub> in the Arthit gas field were in or out of isotopic equilibrium with each other. The results of the plot indicate that carbon isotopic compositions of CO<sub>2</sub> and CH<sub>4</sub> in Arthit gas field are out of isotopic equilibrium. Because of the non-isotopic equilibrium and the sluggishness of the CO<sub>2</sub> - CH<sub>4</sub> gaseous reaction, the carbon isotopic reequilibration between CO<sub>2</sub> and CH<sub>4</sub> in Arthit gas field should not have been undergone to a significant degree. It is therefore likely that the carbon isotopes of both CO<sub>2</sub> and CH<sub>4</sub> do maintain their original isotopic signatures. Hence it is possible to use the  $\delta^{13}\text{C CO}_2$  values to interpret the source of CO<sub>2</sub> as well as the  $\delta^{13}\text{C}$  values of CH<sub>4</sub> for the origin of CH<sub>4</sub> from its own isotopic variation separately. This assumption can be confirmed by the carbon isotopic values of all methane samples (the  $\delta^{13}\text{C CH}_4$  values of 60 samples varying from -26 to -52 ‰, see Figure 15) which fall in a typical range of thermogenic methane even in some gas samples containing small content of CH<sub>4</sub> but large amount of CO<sub>2</sub>. Based on the content and carbon isotopic values of CO<sub>2</sub> the gas reservoirs in Arthit gas field can be grouped as

**Group 1:** High CO<sub>2</sub> composition about 40 to 90% with enriched isotopic values ranging from 0 to 8‰. This group is characterized by inorganic dominated source and may be generated deep buried inorganic sources. This gas migrated along faults and fractures before mixed hydrocarbon gases and accumulated in shallower reservoir.

**Group 2:** This group can be divided into 3 sub categories because it dominated by CH<sub>4</sub> and CO<sub>2</sub> of inorganic, organic (kerogen) and a mixing origins. The CO<sub>2</sub> content of this group ranging from 5 to 40% with  $\delta^{13}\text{C}$  values from 0 to 14‰.

- **Group 2a:** Organic dominated source, very light carbon isotopic value, no contribution of inorganic sources of CO<sub>2</sub> so the CO<sub>2</sub> (organic source) content is very low.
- **Group 2b:** Mixing sources with minor to moderate CH<sub>4</sub> dilution. Low to medium CO<sub>2</sub> contents (5–40%), carbon isotopic values of CO<sub>2</sub> are ranging from -8‰ to -13‰.
- **Group 2c:** This sub-group represents reservoir gases dominated by CH<sub>4</sub> without organic CO<sub>2</sub>. Varying amount of inorganic CO<sub>2</sub> could migrate into such the reservoirs and their carbon isotopic compositions of CO<sub>2</sub> in the reservoirs are controlled essentially by the isotope values of inorganic CO<sub>2</sub>. This sub-group is therefore has the isotopic value similar to inorganic CO<sub>2</sub> which is above -8‰.

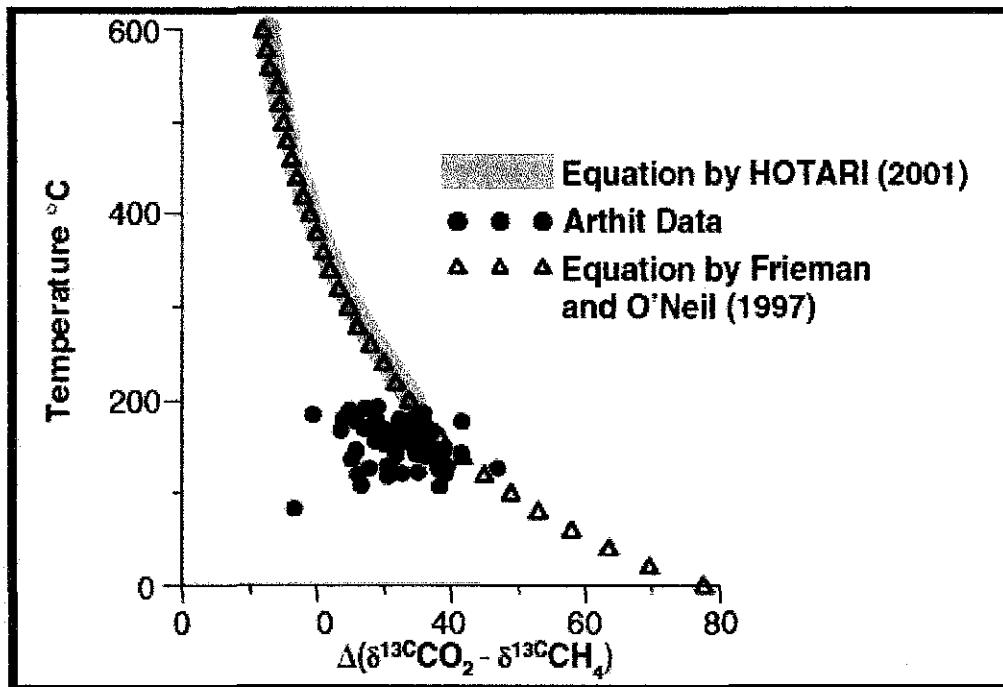


Figure 11: Carbon isotope fractionation factors of CO<sub>2</sub> and

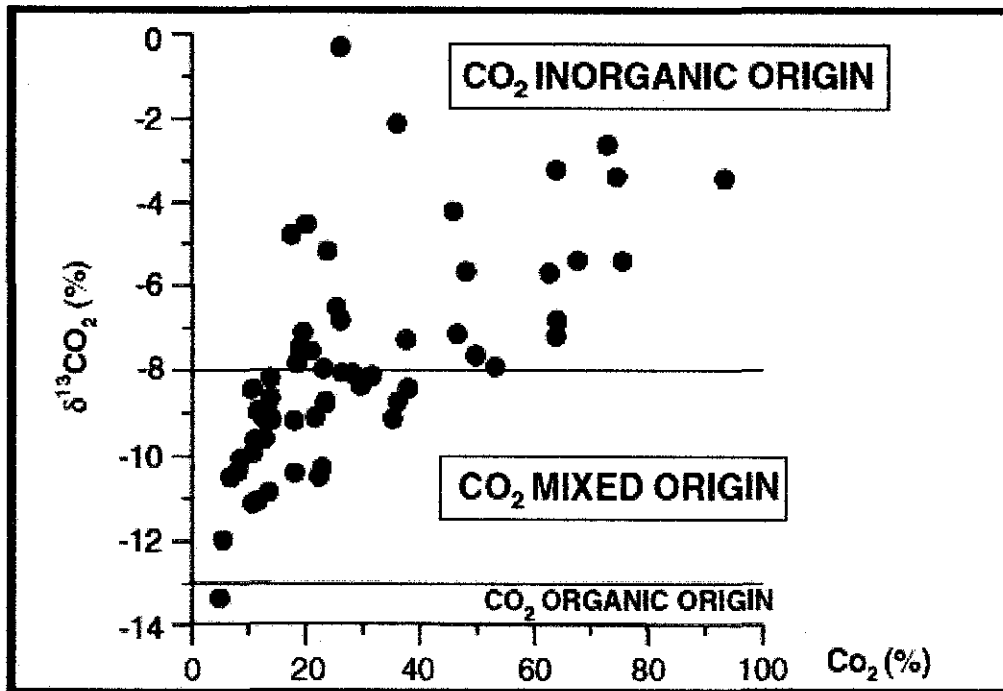


Figure 12: Cross plot between CO<sub>2</sub> contents and carbon

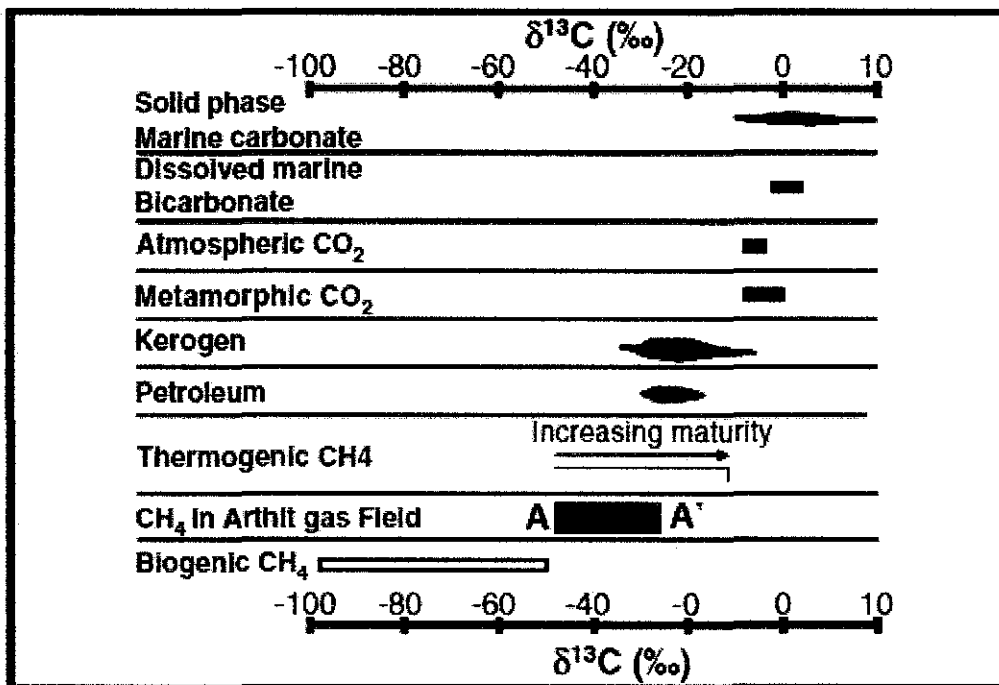


Figure 13: Carbon isotope compositions of major carbon

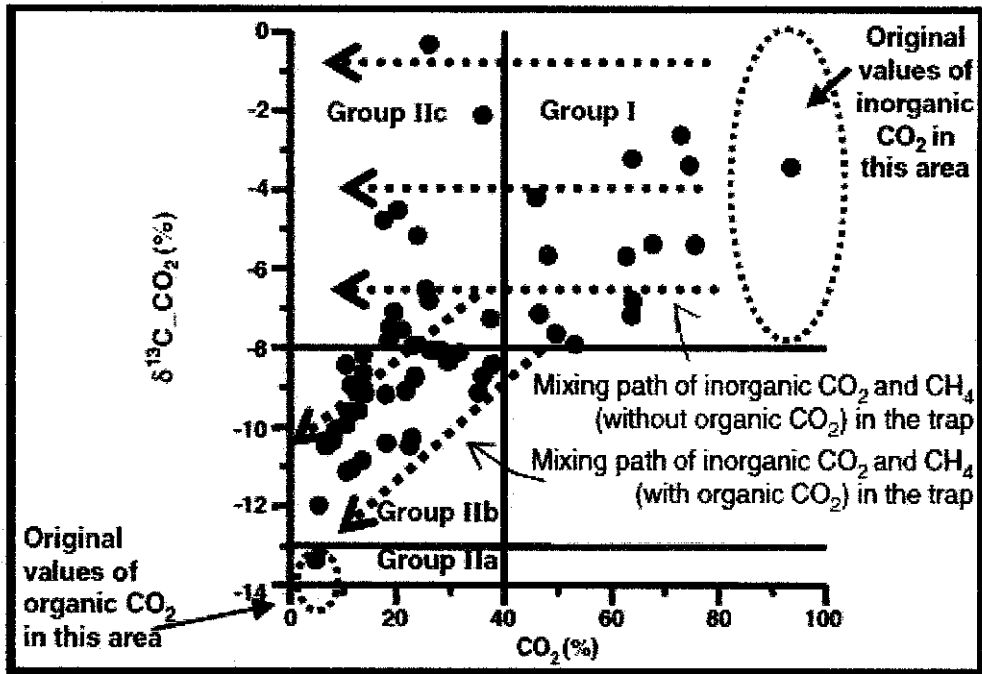


Figure 14: Cross plot between CO<sub>2</sub> contents and Carbon isotopic

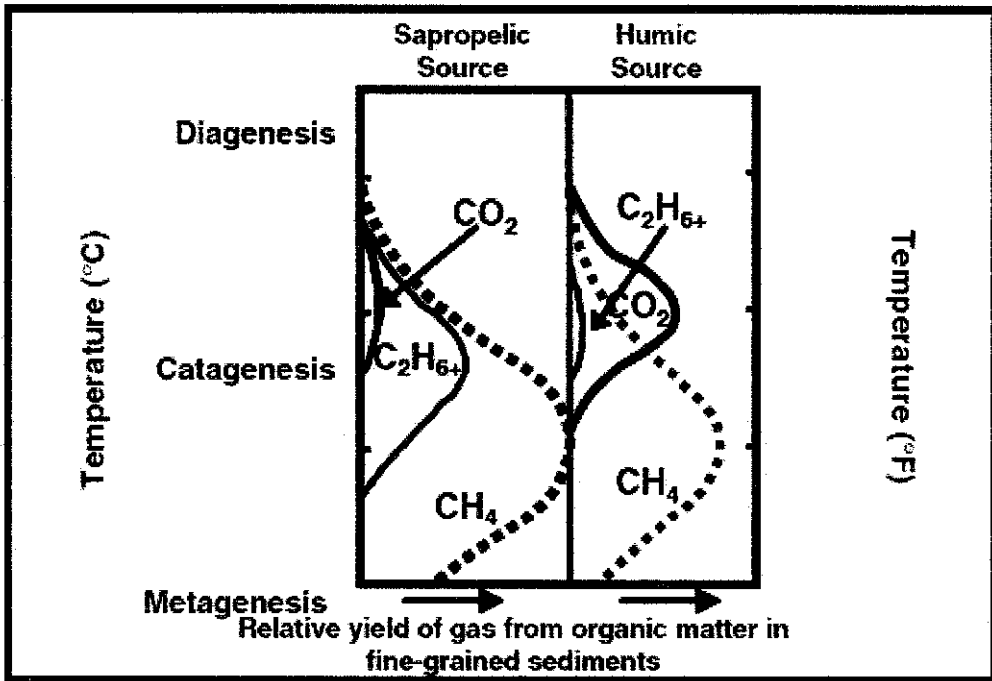


Figure 15: The generation of gases from organic matter with

## **2.7 Possible Inorganic Origin of the High CO<sub>2</sub> Gas Reservoirs in the Platong and the Erawan Gas Fields, Gulf of Thailand (Masashi Fujiwara, Makoto Yamada, Akio Sasaki, 2009)**

The Erawan gas field is located at central part of Thailand Trough in the Gulf of Thailand. Maximum production of carbon dioxide and nitrogen found from northwestern part of Erawan gas field are 59.72%. In this field natural gas are divided into two main groups which are

**Group A:** Characterized by heavy methane ranging from -30 to 33% PDB on carbon isotopic composition and poses high content of carbon dioxide and nitrogen. Gases produce from this group might be originated from organic and inorganic sources. This gas is believed have migrated into reservoirs from Pre-tertiary basement through fault.

**Group B:** This group of gases contains normal content of carbon dioxide and nitrogen and lighter methane (-38 to 41% PDB) by carbon isotopic composition. This gases is a result of thermal maturation and degradation of organic matter in Tertiary sediments.

The Platong gas field was discovered by the Platong-1 well in 1976 and commercial production was initiated in 1985. The clean up tests before production started showed that some production wells were non-commercial due to the presence of high CO<sub>2</sub> in some reservoirs and led the operator to modify the production profile. The origin of the high CO<sub>2</sub> was interpreted to be of hydrothermal origin based on geological phenomenon such as abundance of pyrite in the cuttings and samples of fresh water taken in the tests. E-logs of shale near the high CO<sub>2</sub> shows high density and relatively low neutron porosity. Difference in shale density between high CO<sub>2</sub> zones and normal CO<sub>2</sub> zones is 0.08gm/cc on average. Resistivity of shale zone in high CO<sub>2</sub> zones is relatively higher compared to that of low CO<sub>2</sub> zones due to low salinity water in shales probably derived from hydrothermal origin. (Placeholder1) (Masashi Fujiwara, 2009)

## 2.8 Enhanced Oil Recovery in Malaysia: Making it Reality (M.K Hamdan, ,N. Darman, D. Hussain,Z. Ibrahim)

As in January 2003, Malaysian oil reserves stands at 3.5 BSTB and the cumulative oil production is 4.9 BSTB and oil in place 24.9BSTB. These numbers translate to an average oil recovery factor of 34%. PETRONAS has set target to increase the recovery factor the existing 34% - 45%. One of the ways to achieve this objective is through EOR in the depleted oil fields.

The earliest feasibility study for EOR in Malaysia was recorded in 1985 with objective to investigate the technical potential of miscible enriched gas and surfactant flooding in the fields located in Peninsular Malaysia. Then in 1986, a screening study was conducted by Shell to look into EOR potential in the East Malaysia. The study of recognizing the potential of enhanced oil recovery in the fields is conducted later by PETRONAS in 2000. From Peninsular Malaysia 33 reservoirs is screened from 16 fields and 39 reservoirs from 19 fields in East Malaysia. By considering some practical limitation (gas source and reservoir heterogeneity) the number was reduced to 37 reservoirs. The main processes studied in the screening exercise were chemical, microbial enhanced oil recovery and gas flooding. The miscible hydrocarbon and CO<sub>2</sub> WAG flooding are the most favorable method.

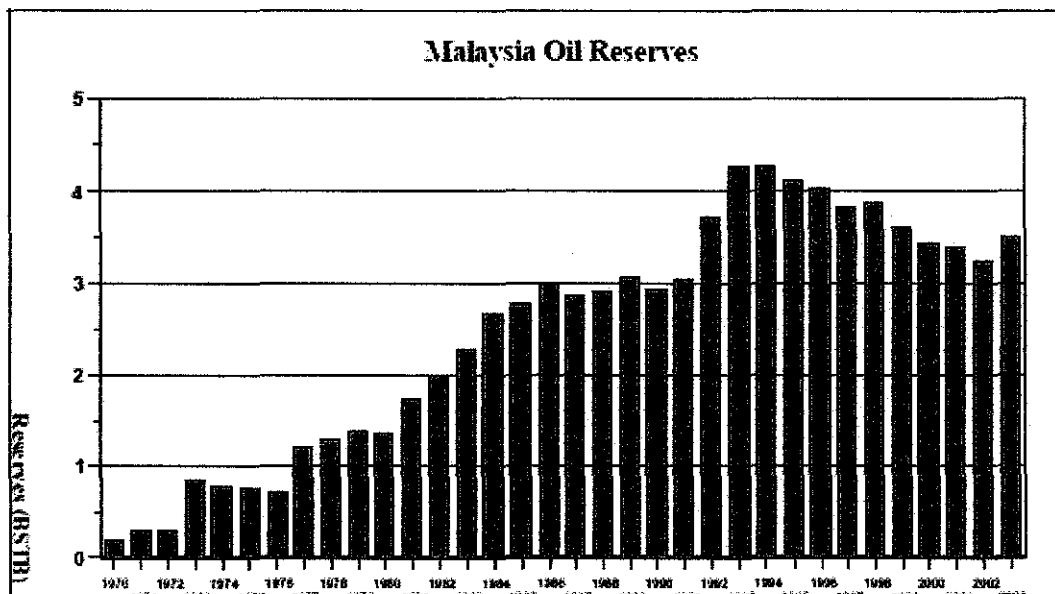


Figure 16: Oil reserves in Malaysia

### **2.8.1 Challenges and Obstacles**

In Malaysia, most of producing fields are located offshore. In this environment, technical and commercial value needs to be identified precisely. One of the primary concerns is the well spacing for effective EOR process. The average well spacing for the Malaysian fields ranges from 100ft-3000ft. This distance is not suitable for chemical and thermal process which requires much closer well spacing. But this range of this is suitable for gas flooding mechanism as this method operated at larger well spacing. However large spaced wells caused a difficulty in prediction of recovery due to uncertainty of the reservoir characteristics between wells.

Nature of the well itself will add another complexity in implementing EOR in Malaysian. Most of the well is deviated or highly deviated or without proper flooding pattern. For a conversion to a pattern injector, some wells need to be sidetracked in order to optimize the injection capability. This action will increase the cost for EOR implementation. Age of the offshore platform is another concern in EOR implementation. On the average 68% of 157 existing platforms are more than 20 years old. Large investment needed to maintain the existing platforms and installation of compressor and pumps is required for EOR projects.

The main obstacle for EOR implementation in offshore is the high cost and also the technology itself. Below figure expressed the average costs of the difference types of recovery process.

Process	Cost, US\$/bbl of incremental oil	
	Injectant Only	Total Process*
Thermal - Steam - Purchased fuel	3 - 5 4 - 6	5 - 7 7 - 10
Gas - CO <sub>2</sub>	5 - 10	12 - 20
Chemical - Surfactant (Micellar) - Alkaline - Surfactant/Alkaline/Polymer - Polymer	10 - 20 ~ 7 2 - 7 1 - 5	20 - 30 ~ 19 10 - 17 ~ 2 - 7

## 2.9 Enhanced Oil Recovery in Malaysia: Making it Reality Part 2 (Y. Samsudin, N. Darman, D. Husain, M.K Hamdan, PETRONAS Carigali Sdn Bhd, 2005)

Among the Enhanced Oil Recovery (EOR) techniques applicable to Malaysian reservoirs, CO<sub>2</sub> injection has been identified as the most amenable process. Preliminary laboratory studies were conducted on the applicability of CO<sub>2</sub> displacement process. It is estimated that potentially, about 1 billion barrel additional crude oil could be recovered from Malaysian producing oil fields through application of IOR/EOR. Such a gain will result in reserves growth, and extend the producing life of these reservoirs. This potential for oil recovery presents a major economic opportunity. In Malaysia there are several EOR projects that are in the late stages of study which being used as references for this particular study.

### 2.9.1 Dulang Field (Immiscible WAG)

This field located at about 130 km from Terengganu Crude Oil Terminal (TCOT). Dulang structures are East West trending anticline with area size about 11km by 3.5 km. The field was divided into three major areas namely Dulang Unit, Dulang Western and Dulang Eastern. As time goes by reservoir pressure depleted and led to declining of production rates. Later, feasibility studies identified reinjection of the produced gas as EOR option. For EOR operation WAG method was proposed and now at its final stage

of implementation. Soon after WAG injection started, pressure increase with increase oil rate and reduced GOR and water cut. Oil rate increase to 300 BOPD from 105 BOPD while GOR reduced to 200 scf/stb from 4500 scf/stb and water cut reduced from 80% to 70%.

### **2.9.3 West Lutong Field**

West Lutong is located in the Baram Delta Province 12 km North West offshore Lutong. The KL and MN sand are the major producing reservoirs West Lutong and contribute more than 70 % of the total production. The STOIP is 110 MMstb. A test was conducted to test the feasibility of miscible gas injection in Baram Delta fields. The current plan is to implement an observation pilot program with one injector and one or two observation well to be drilled 100 feet away. 2MMscf/d of high purity CO<sub>2</sub> will be used to supply the injectant gas at miscibility conditions. Continuous gas injection is considered due to the extremely strong aquifer and the process will be closely monitored to see the performance of pilot program. If the pilot is successful, the miscible process can give an incremental of up to 165 MMstb for the BDO fields.

## **3.0 Petex (Petroleum Experts)**

### **3.0.1 MBAL**

Efficient reservoir development requires a good understanding of reservoir and production systems. MBAL helps the engineer better define reservoir drive mechanisms and hydrocarbon volumes. This is a prerequisite for reliable simulation studies. This software is commonly used for modeling the dynamic reservoir effects prior to building a numerical simulator model. It also contains the classical reservoir engineering tool and has redefined the use of Material Balance in modern reservoir engineering. For existing reservoirs, MBAL provides extensive matching facilities. Realistic production profiles can be run for reservoirs with or without history matching. MBAL is an intuitive

program with a logical structure that enables the reservoir engineer to develop reliable reservoir models quickly.

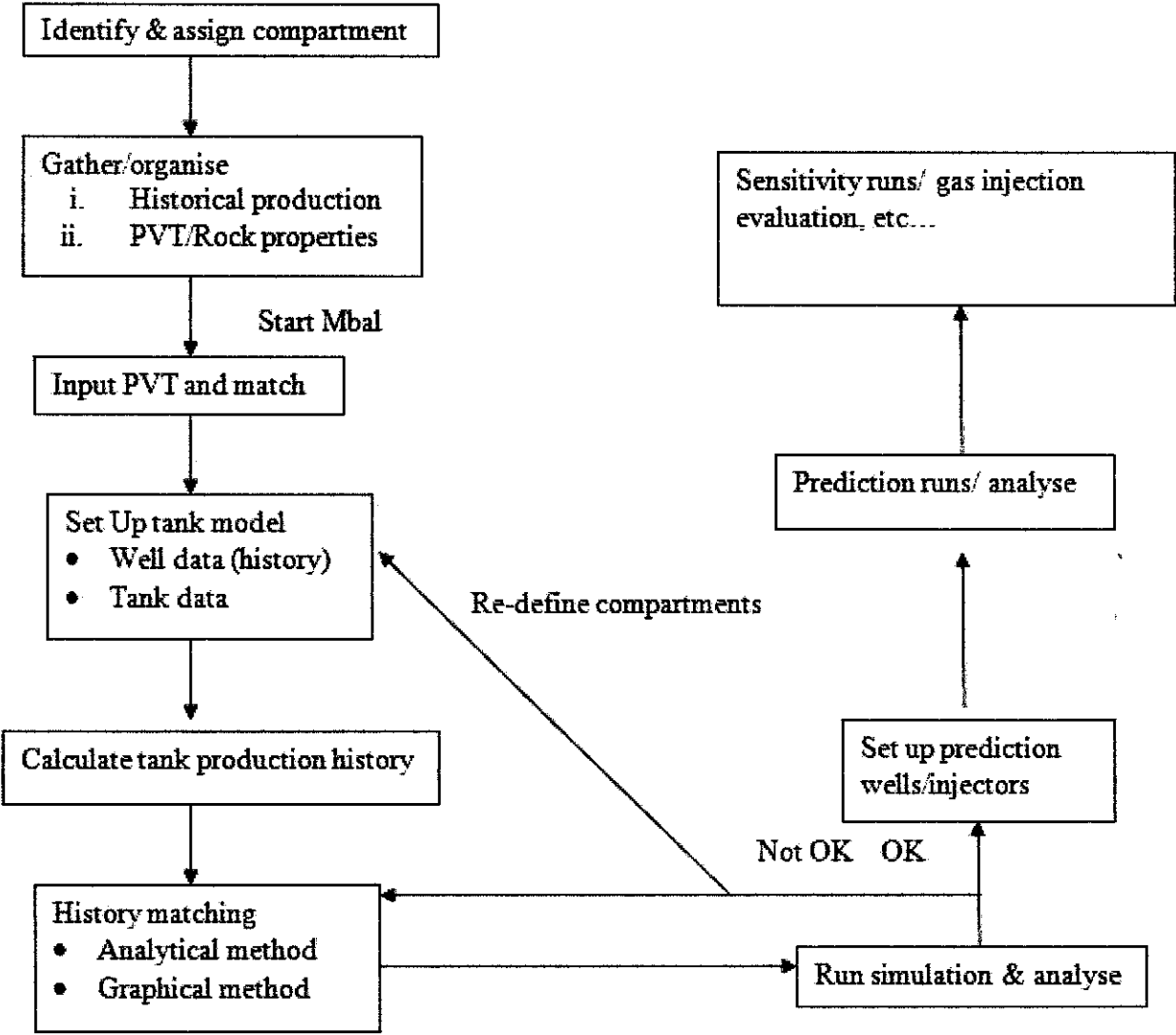


Figure 17: Mbal workflow

**3.0.2 PROSPER**

PROSPER is a well performance, design and optimization program for modeling most types of well configurations found in the worldwide oil and gas industry today. This application can assist the production or reservoir engineer to predict tubing and pipeline hydraulics and temperatures with accuracy and speed. It’s sensitivity calculation

features enable existing well designs to be optimized and the effects of future changes in system parameters to be assessed. PROSPER is designed to allow building of reliable and consistent well models, with the ability to address each aspect of well bore modeling; PVT (fluid characterization), VLP correlations (for calculation of flow line and tubing pressure loss) and IPR (reservoir inflow). By modeling each component of the producing well system, the User can verify each model subsystem by performance matching. Once a well system model has been tuned to real field data, PROSPER can be confidently used to model the well in different scenarios and to make forward predictions of reservoir pressure based on surface production data. With PROSPER detailed flow assurance can be studied at well and surface pipeline level. This software provides unique matching features which tune PVT, multiphase flow correlations and IPR to match measured field data, allowing a consistent model to be built prior to use in prediction (sensitivities or artificial lift design).

### **3.1 Material Balance Principle**

When a volume of oil is produced from a reservoir, the space once occupied by this volume must be filled by something else. This could be replaced by either;

- Gas cap expansion
- Released gas volume
- Remaining oil volume
- Rock and water expansion
- Net water influx

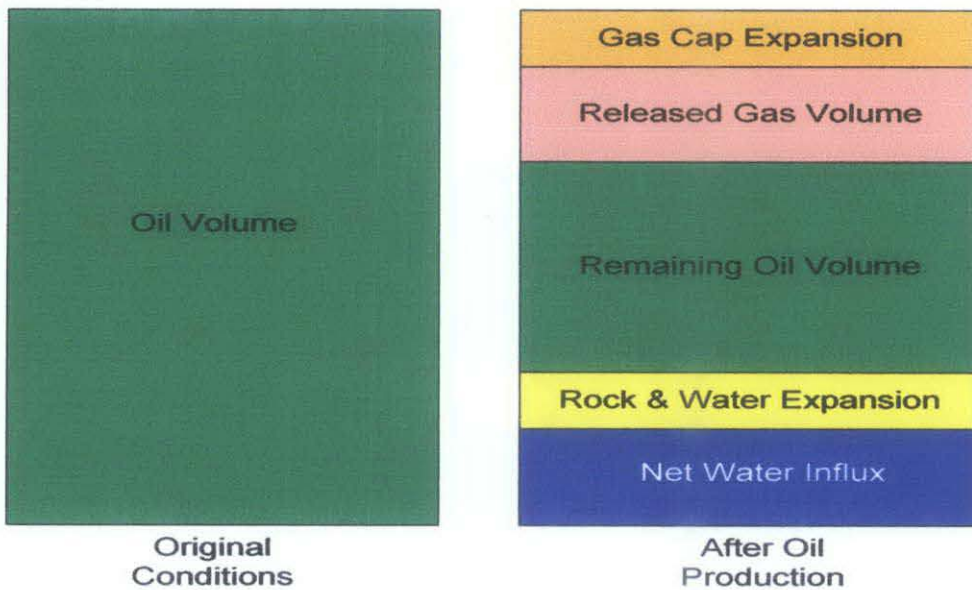


Figure 18 : Material Balance Principle

### 3.1.1 Gas Cap Expansion

- Gas cap (if present) will expand to partially replace the volume occupied by the produced oil.

$$\text{GAS CAP EXPANSION} = (G - G_{PC}) B_G - G_{PC} B_{GI} \text{ [rb]}$$

Where

$G$  = original gas cap gas volume, scf

$G_{PC}$  = cumulative gas production from the gas cap, scf

$B_G$  = gas formation volume factor at current pressure, rb/scf

$B_{GI}$  = gas formation volume factor at original reservoir pressure, rb/scf

- gas cap shrinkage problem
  - if  $G_{PC}$  is large
  - loss of oil recovery

### 3.1.2 Release gas volume

- gas will be released from solution if reservoir pressure falls below the bubble point

At any time during the production of a reservoir, the gas originally in solution can be placed into three categories

- still in solution
- released from solution and produced from reservoir
- released from solution but still in reservoir

$$\text{RELEASED GAS VOLUME} = \{N R_{SI} - (N - N_P) R_S - G_{PS}\} B_G \text{ [RB]}$$

$N$  = original oil volume, STB

$N_P$  = cumulative oil produced, STB

$G_{PS}$  = cumulative solution gas produced, SCF

$R_{SI}$  = original solution GOR, SCF/STB

$R_S$  = solution GOR at current pressure, SCF/STB

$B_G$  = gas formation volume factor at current pressure, RB/SCF

### 3.1.3 Remaining Oil Volume

$$\text{RESERVOIR OIL VOLUME} = (N - N_P) B_O \text{ [RB]}$$

Where;

$N$  = original oil volume, STB

$N_P$  = cumulative oil produced, STB

$B_O$  – oil formation volume factor at current pressure, RB/STB

### 3.1.4 Rock and Connate Water Expansion

- effect is generally negligible if gas phase is present

- effect is important only when  $P > P_B$  in oil reservoirs
- expansion effects are combined into one term and expressed as the formation compressibility,  $C_f$  – fractional change in hydrocarbon pv per psi change in reservoir pressure
- PV can be expressed in terms of original oil volume

$$\text{ORIGINAL OIL VOLUME} = N B_{OI} = V_P S_{OI} = V_P (1 - S_{WI}) \quad [RB]$$

where:

$N$  = original oil volume, STB

$B_{OI}$  = OIL formation volume factor at initial pressure, RB/STB

$V_P$  = reservoir pore volume, RB

$S_{OI}$  = initial oil saturation

$S_{WI}$  = initial or connate water saturation

$$\text{Rock expansion} = C_f \left( \frac{N B_{OI}}{1 - S_{WI}} \right) (P_i - P) \quad [RB]$$

$C_f$  = formation compressibility, vol/vol/psi

$P_i$  = initial reservoir pressure, psi

$P$  = current reservoir pressure, psi

### 3.1.5 Water Influx

- cannot be calculated directly
- depends on size and strength of aquifer
- can calculate net water influx indirectly

$$\text{NET WATER INFLUX} = W_E - W_P B_W \quad [RB]$$

Where;

$w_e$  = cumulative water influx, RB

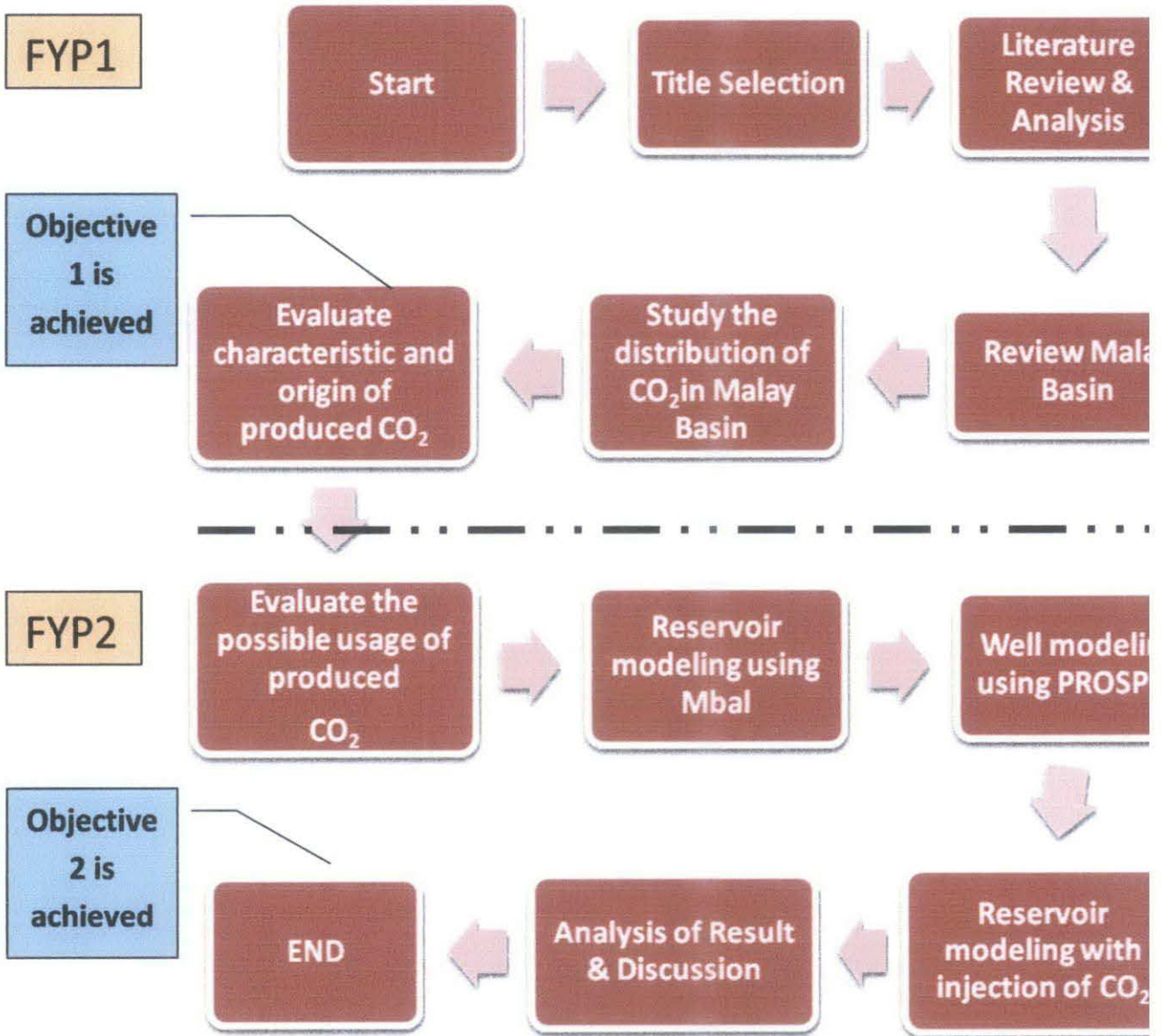
$w_p$  = cumulative water produced, STB

$b_w$  = water formation volume factor at current pressure, RB/STB

# CHAPTER 3

## METHODOLOGY

### 3.1 Methodology Flowchart



### 3.3 Distribution of CO<sub>2</sub> in Malay Basin

The author used the data from The Petroleum and Geology Resources book as the references data for the production of CO<sub>2</sub> in the Malay Basin. From Figure. 15 illustrates that the high production of CO<sub>2</sub> concentrated mainly in the center and the northern part of the Malay Basin. The percentage of CO<sub>2</sub> ranges from approximately 5% to 85% mol. The percentage of CO<sub>2</sub> in Malay Basin is coutoured to see the trend of it.

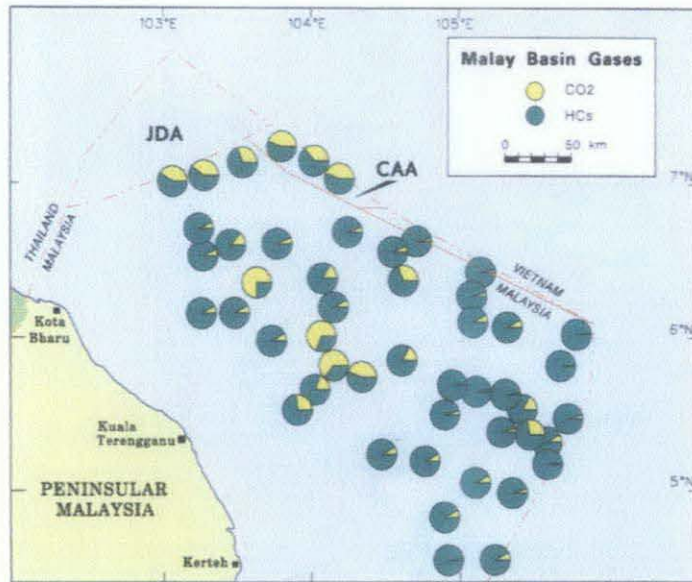


Figure 19 : Distribution of CO<sub>2</sub> in the Malay Basin (The Petroleum Geology and Resources of Malaysia, 1999)

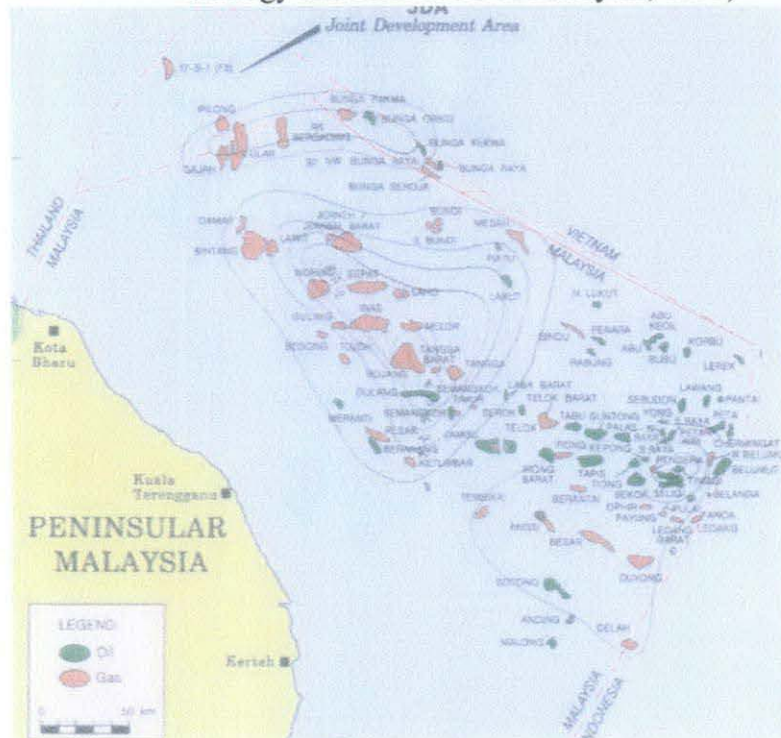


Figure 20 : Contour map of CO<sub>2</sub> distribution (The Petroleum Geology and Resources of Malaysia, 1999)

From the percentage of CO<sub>2</sub> counted we can see that there are three main pockets where the CO<sub>2</sub> are concentrated, which are north, center and south part of the basin. The Malay Basin basement are found deeper in the north and axial. Buried deeper in the basin, the geothermal gradient increase and this phenomena is prove by referring to thermal gradient of Malay Basin in Figure 7 and 8. This condition is ideal for generation of inorganic CO<sub>2</sub> from thermal breakdown of carbonates which occur at high temperature. For this study the author are focusing on finding the source of high production of CO<sub>2</sub> which mostly results from inorganic origin. This is because this type of CO<sub>2</sub> is a stable source compare to organic origin of CO<sub>2</sub> which results from breakdown of keroge at low temperature. This type of CO<sub>2</sub> are found concentrated in the center of the basin and associated with large gas accumulation. This gas are migraed along the fault and mixed with the shallower thermal gas. Such phenomena is found in Dulang and Tangga fields.

### **3.4 CO<sub>2</sub> flooding modeling**

In designing effective CO<sub>2</sub> flooding, there are rule of thumbs that should be follow

- To be an effective solvent, CO<sub>2</sub> must flow through the reservoir above its minimum miscibility pressure (MMP). This means that the reservoir generally should be greater than 2,500 ft. deep.
- CO<sub>2</sub> is most effective with light crudes, those with oil gravities greater than 25° API. Preferably higher than 30 ° API (William C. Lyons, Gary J. Plisga, (William C. Lyons, 2005))
- Because CO<sub>2</sub> flows through the reservoir more easily than oil, it also does best in reservoirs with low heterogeneity. If some layers of the reservoir are far more porous than others, CO<sub>2</sub> will flow there preferentially, rather than maintaining uniform front and high sweep efficiency.
- Stratification, fracturing and adjacent loss zones (adjacent gas caps) can cause loss of CO<sub>2</sub> and reduced oil recovery.

### 3.4.1 Reservoir modeling

Reservoir modeling is important to simulate the real scenario of the reservoir by using fictitious data obtain from well report. The detail modeling process is explained in the appendix.

#### Data preparation

For this modeling there are numbers of data required to run the software such as PVT data, reservoir data, well data and etc. However due to lack of data, the author will used the fictitious data to run the software. These data should be recalculated once the actual information's are available.

#### PVT data

Reservoir Pressure : 2136.3 psi  
Reservoir Temperature : 155 deg F  
Formation GOR : 336 scf/STB  
Oil Gravity : 30 API  
Water Salinity : 30000 ppm

#### Reservoir data

Original Gas in Place : 72.135 MMSTB  
Porosity : 0.25 %  
Relative Permeability :

	Residual Fraction	End Point	Exponent
K <sub>rw</sub>	0.206	0.68	0.8
K <sub>ro</sub>	0.01	0.78	1
K <sub>rg</sub>	0.01	0.5	2

Table 4 : Relative permeability

### **Reservoir definition**

There are numbers of tool that can be used to define the reservoir engineering analysis tool and for this particular study, material balance analysis tool is selected. Material balance is based on the principle of the conservation mass which is:

Mass of fluids originally in place = fluids produced + remaining fluids in place

### **PVT correlations matching**

In order to accurately predict both pressure and saturation changes throughout the reservoir, it is important that the properties of the fluid are accurately described. The ideal situation would be to have data from laboratory studies done on fluids samples. As this is not always possible, the correlations matching method is used. The matching process is used to adjust the empirical fluid property correlations to fit measured PVT laboratory data. Correlations are modified using non-linear regression technique to best fit measure data. From the correlations matching (see appendix) Standing and Beal et al has been selected has been chosen as it is the best correlation compares to other correlations.

### **3.4.2 Well modeling**

Petroleum Experts (PROSPER) is used to model the producer well.

Firstly the well system is defined as summarized below:

Fluid type : Oil and water  
PVT method : Black oil  
Separator : Single stage separator  
Flow type : tubing flow  
Well type : producer  
Completion : cased hole  
Gravel pack : no

## **PVT correlation matching**

PVT data derived from well test report is used to be matched with PROSPER model. This process is important to select the best correlation to simulate vertical flow performance (VFP) and also for nodal analysis run. From the correlation matching (see Appendix) Glaso\* and Beal Chew et al\* has been chosen as the PVT correlation for Inas as it is the best compares to other correlation.

## **IPR prediction**

For IPR prediction, the data from reservoir modeling were used.

Reservoir pressure	: 2151.0 psi
Bottomhole temperature	: 155°F
Water cut	: 0 %
Total GOR	: 267 scf/STB
Oil Gravity	: 33API
Gas Gravity	: 0.65
Water Salinity	: 30000 ppm

Since the reservoir pressure is greater than the bubble point the reservoir is considered as under saturated reservoir and therefore Vogel's model is used. This model generates PI (Productivity Index) equal to 3.91 STB/day/psi with absolute open flow (AOF) of 4649.0 STB. To check the validity of calculated IPR, the well test data is used to match with the IPR plot (see appendix).

## **Vertical Flow Correlation Matching**

To select the best correlation to represent the outflow, a few vertical flow correlation have been selected and simulated to derive the pressure traverse that best match the measured pressure-depth data from well test report.

Figure A (appendix) illustrates the pressure profile calculated for each correlation and how they matched the measured data. Francher & Brown correlation has been used as a reference profile since it represents a non-slip vertical flow condition.

### **Injector Well**

Since there is no details information on CO<sub>2</sub> flooding operations, the FWBHP of the injector well is assumed to be constant at 2200psia. The maximum gas injector rate is assumed at 6MMscf/day. Well injector performance is attached in the appendix

## CHAPTER 4

### RESULTS AND DISCUSSION

#### 4.1 CO<sub>2</sub> genetic relation

Based on recent study of CO<sub>2</sub> distribution in Malay Basin, high occurrence of CO<sub>2</sub> concentrated at northern and central region of the basin (Figure 17). The highest concentration of CO<sub>2</sub> recorded is approximately 78 mol% and the lowest reading is about 5%.

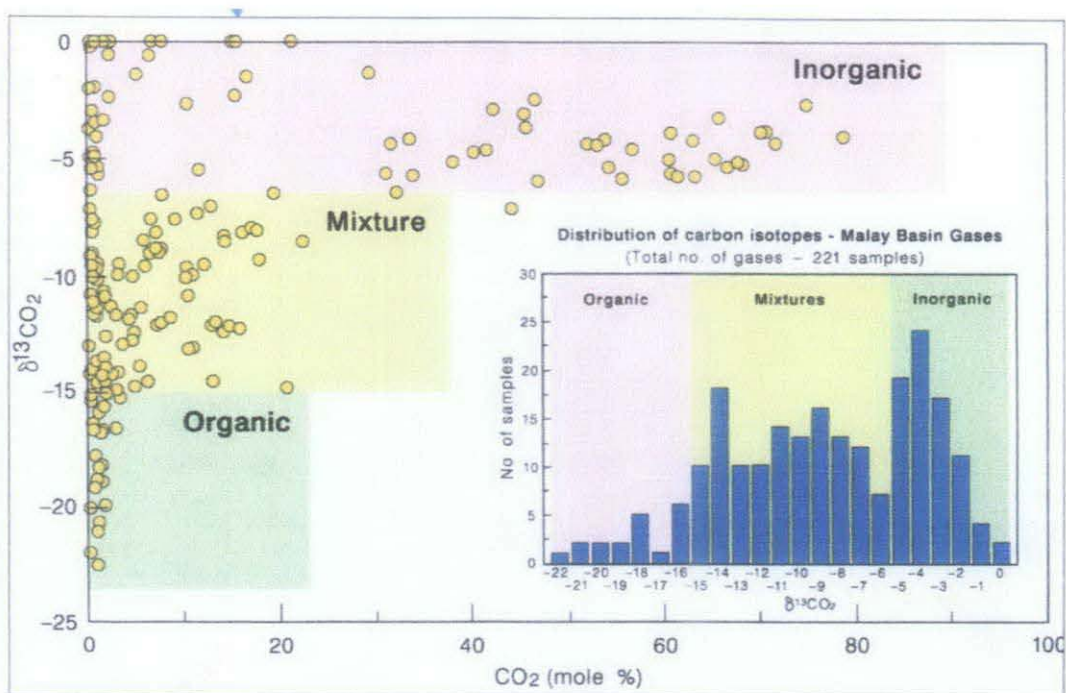


Figure 21: Cross plot of  $\delta^{13}\text{C}$  against mole % for CO<sub>2</sub> in Malay Basin (The Petroleum Geology and Resources of Malaysia, 1999)

Figure above indicate that high percentage of CO<sub>2</sub> production originates from inorganic which is generally probably resulting from the thermal metamorphism of carbonates in

the pre-Tertiary basement. In these gases, isotopes values range from 0-5%. These gases are found concentrated in the center of basin and associated with large gas accumulation. The isotopic value of organic derived CO<sub>2</sub> ranges from -15 to 25% and the distribution not more than 25% mol of total gas distribution.

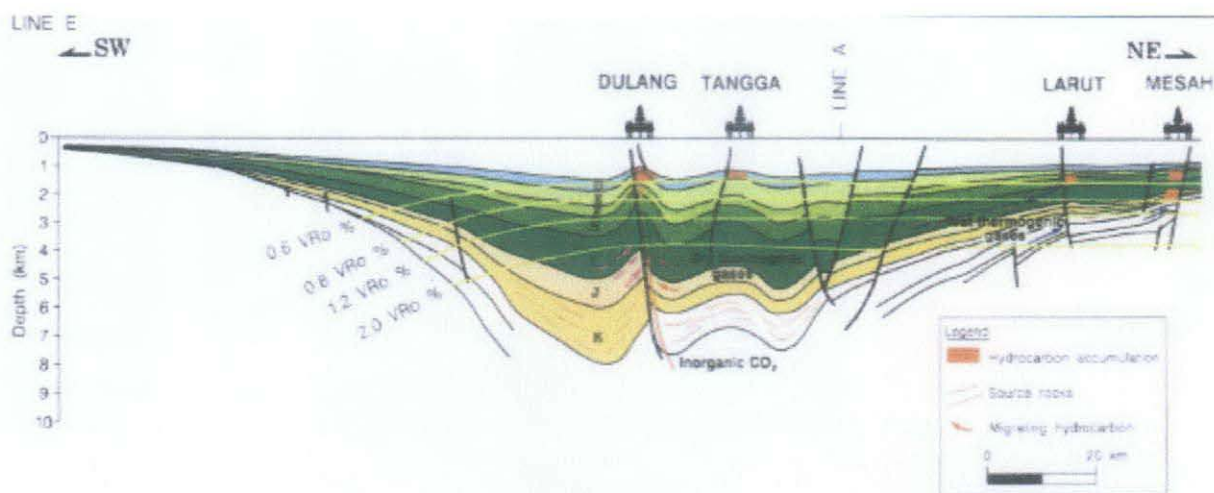


Figure 22 : CO<sub>2</sub> migration route (The Petroleum Geology and Resources of Malaysia, 1999)

The produced gas migrated along the fault and mixed with shallower thermally generated gas. This phenomenon explains the presence of carbon dioxide in groups E and younger gas which is mainly confined to the axis of the basin.

#### 4.2 Results from modeling

Without the assistance of CO<sub>2</sub> flooding, the oil production rate only last until 2018 as shown in below figure.

Time	Tank Pressure	Oil Rate	Gas Rate	Water Rate	Liquid Rate	Gas Inj Rate	Water Inj Rate	Gas Lift Rate	Gas Rec. Rate	Wal Rec. Rate	Aqu Water Rate	Gas Gas Cap Rate	Avg G Inj Ra
date m/d/y	psig	STB/day	MMscf/day	STB/day	STB/day	MMscf/day	STB/day	MMscf/day	MMscf/day	STB/day	STB/day	MMscf/day	MMscf/
09/11/2016	1269.21	1392.67	4.59162	24.5595	1417.23	0	0	0	0	0	0	0	0
12/11/2016	1240.93	1297.09	4.33223	23.5275	1320.62	0	0	0	0	0	0	0	0
03/12/2017	1214.1	1203.72	4.06952	22.411	1226.13	0	0	0	0	0	0	0	0
06/11/2017	1192.89	1129.41	3.84248	21.4185	1150.83	0	0	0	0	0	0	0	0
09/10/2017	1177.48	1074.22	3.65485	20.5922	1094.81	0	0	0	0	0	0	0	0
12/10/2017	1162.57	1020.09	3.47114	19.76	1039.85	0	0	0	0	0	0	0	0
03/11/2018	1148.17	967.539	3.29302	18.9324	986.471	0	0	0	0	0	0	0	0
06/10/2018	1136.58	914.07	3.12811	18.1871	932.282	0	0	0	0	0	0	0	0

Figure 23: Reservoir production (without CO<sub>2</sub> flooding)

When the CO<sub>2</sub> injection is implemented to the reservoir, the oil production is increase until 2026. There is almost 20% of increase in production rate in comparison to the natural flow. Details graph is attached in the appendix.

Done X Cancel ? Help Report Layout Plot Calc Save

Stream Prediction

Time	Tank Pressure	Oil Rate	Gas Rate	Water Rate	Liquid Rate	Gas Inj Rate	Water Inj Rate	Gas Lift Rate	Gas Rec. Rate	Wat Rec. Rate	Aqu Water Rate	Gas Gas Cap Rate	Avg Gas Inj Rate	Avg Water Inj Rate
date m/d/y	psig	STB/day	MMscf/day	STB/day	STB/day	MMscf/day	STB/day	MMscf/day	MMscf/day	STB/day	STB/day	MMscf/day	MMscf/day	STB/day
09/17/2019	1198	1114.29	4.11223	18.9159	1133.19	5.67241	0	0	0	0	0	0	5.68737	0
12/17/2019	1192.41	1130.16	4.22425	18.7727	1148.93	5.64934	0	0	0	0	0	0	5.66257	0
03/17/2020	1196.29	1144.1	4.33016	18.6052	1162.7	5.62903	0	0	0	0	0	0	5.64066	0
06/16/2020	1199.66	1156.28	4.43033	18.4177	1174.7	5.61126	0	0	0	0	0	0	5.62143	0
09/15/2020	1204.13	1172.29	4.53791	18.2487	1190.53	5.5877	0	0	0	0	0	0	5.60156	0
12/15/2020	1208.02	1186.24	4.63866	18.0576	1204.3	5.56711	0	0	0	0	0	0	5.5788	0
03/16/2021	1211.2	1197.68	4.73156	17.8451	1215.53	5.55024	0	0	0	0	0	0	5.5598	0
06/15/2021	1213.74	1206.88	4.81728	17.616	1224.5	5.53671	0	0	0	0	0	0	5.54434	0
09/14/2021	1215.71	1214.07	4.8964	17.3744	1231.44	5.5262	0	0	0	0	0	0	5.5321	0
12/14/2021	1217.17	1219.46	4.96348	17.1236	1236.58	5.5184	0	0	0	0	0	0	5.52274	0
03/15/2022	1218.17	1223.24	5.03639	16.8652	1240.11	5.51303	0	0	0	0	0	0	5.51597	0
06/14/2022	1218.77	1225.59	5.09393	16.6046	1242.19	5.50884	0	0	0	0	0	0	5.51153	0
09/13/2022	1219	1226.65	5.15708	16.3405	1242.99	5.5066	0	0	0	0	0	0	5.50917	0
12/13/2022	1218.91	1226.57	5.21043	16.0754	1242.65	5.50609	0	0	0	0	0	0	5.50867	0
03/14/2023	1218.53	1225.48	5.25978	15.8105	1241.29	5.51112	0	0	0	0	0	0	5.50982	0
06/13/2023	1217.3	1223.49	5.30546	15.5487	1239.03	5.51451	0	0	0	0	0	0	5.51242	0
09/12/2023	1217.04	1220.7	5.34775	15.2849	1235.98	5.5191	0	0	0	0	0	0	5.51633	0
12/12/2023	1215.98	1217.2	5.38632	15.0256	1232.23	5.52474	0	0	0	0	0	0	5.52137	0
03/12/2024	1214.75	1213.09	5.42322	14.7694	1227.86	5.53131	0	0	0	0	0	0	5.52741	0
06/11/2024	1213.37	1208.44	5.45688	14.5157	1222.96	5.53868	0	0	0	0	0	0	5.53432	0
09/10/2024	1211.85	1203.31	5.48812	14.2676	1217.58	5.54675	0	0	0	0	0	0	5.54199	0
12/10/2024	1210.22	1197.78	5.51713	14.0225	1211.8	5.55541	0	0	0	0	0	0	5.55031	0
03/11/2025	1208.5	1191.89	5.54409	13.7816	1205.67	5.56458	0	0	0	0	0	0	5.55919	0
06/10/2025	1206.68	1185.7	5.56917	13.5448	1199.24	5.57418	0	0	0	0	0	0	5.56855	0
09/09/2025	1204.8	1179.24	5.59254	13.3124	1192.56	5.58414	0	0	0	0	0	0	5.5783	0
12/09/2025	1202.96	1172.59	5.61432	13.0843	1185.66	5.59439	0	0	0	0	0	0	5.58839	0
02/03/2026	1201.64	1169.44	5.62388	12.9805	1182.42	5.59921	0	0	0	0	0	0	5.5968	0

Filter

Figure 24: Reservoir production (with CO<sub>2</sub> flooding)

The mechanism of CO<sub>2</sub> flooding can be explained by following sequence. When carbon-dioxide is injected into an oil reservoir, it mixes readily with the residual crude oil. The solubility increases further when the carbon-dioxide is compressed and the oil contains lesser hydrocarbons (low-density). At one point, the miscibility of carbon-dioxide and oil stops. As the temperature increases (and the CO<sub>2</sub> density decreases), or as the oil density increases (as the light hydrocarbon fraction decreases), the minimum pressure needed to attain Oil/ CO<sub>2</sub> miscibility increases. Therefore, when the injected CO<sub>2</sub> and residual oil are miscible, the physical forces holding the two phases apart disappears.

This enables the CO<sub>2</sub> to displace the oil from the rock pores, pushing it towards a producing well just as a cleaning solvent would remove oil from your tools.

## CHAPTER 5

### CONCLUSION

In this study, the authors have studied the distribution of CO<sub>2</sub> and its genetic relation in Malay Basin. From the study it can be concluded that high productions of CO<sub>2</sub> probably resulted from cracking of carbonate at the basement. This is proven by the existence of carbonate rocks such as Kodiang and Setul limestone which buried deeper in Permian and Silurian age respectively. The carbonate cracking process is assisted by the geothermal gradient and heat flow which is predicted in the axis and north region of Malay Basin (refer Figure 9 and Figure 10). The inorganic CO<sub>2</sub> is believe migrated along the fault before accumulated with reservoir and comingle with shallow depth thermogenic gas. This phenomenon explains the high production of carbon dioxide in the central and north region of Malay Basin (noticeably at Dulang and Tangga).

For the EOR program, CO<sub>2</sub> flooding is the suitable candidate to be implemented to increase the production of declining well nearby. With the assistance of the CO<sub>2</sub> the oil production is increase up to 20% from naturally flow. However, this particular modeling didn't take the cost into account. The costs vary depending on filed area, pattern spacing, location, and existing facilities. The separation and transportation of CO<sub>2</sub> also is the major challenge in CO<sub>2</sub> flooding project from its source to point of injection with the required quality. The pipelines, injection and production facilities should be able to withstand the corrosive nature of the CO<sub>2</sub> and high pressure. But in general, total operating expenses range within 10.25\$US/BOE (according to PERMIAN Basin CO<sub>2</sub> flood in 1995). The amount of CO<sub>2</sub>/oil ratios vary from around 26MSCF per barrel produced.

Due to low value of STOIP in Inas field, the EOR program is not economical to implemented to extract the remaining oil in the field. However, CO<sub>2</sub> produced in Inas field can be used to nearby oil field for their field development program.

## REFERENCES

- (PETRONAS), P. N. (1999). Malay Basin. In P. A. Mazlan B Hj Madon, *The Petroleum and Geology Resources of Malaysia* (pp. 173-211). Petroliaam Nasional Berhad (PETRONAS).
- A.A.M Yassin, U. (1988). Enhanced Oil Recovery in Malaysia. *SPE 17693* .
- Azaman Ikhsan, S. a. (1997). The CO2 flooding :Prspect nd challenges on Malaysia oil field. 387,388,389.
- Dewanto Odeara Kartikasurja, S. H., & Tan Giok Lin, M. W. (n.d.). Co2 Capture in mature oil reservoir. *SPE 94181* .
- John P. Lockwood, R. W. (2010). *Volcanoes: Global Perspectives*. Blackwell Publisher.
- Kartikay Sonraza, A. A. (1995). Development and Management of Complex Dulang (E14) Reservoir, Ofshore Malaysia: A simulation Case Study. *SPE 30146* .
- M.A. Barrufet, A. B. (1997-2001). Analysis of the storage capacity for CO2 sequestration of a depleted gas condensate reservoir and saline aquifer.
- M.K Hamdan, N. .. (2004). Enhanced Oil Recovery in Malaysia: Making it Reality. *SPE 93329* .
- Mashashi Fujiwara, M. Y. (2009). Possible Inorganic Origin of the High CO2 Gas Reservoirs in the Platong and the Erawan Gas Fields, Gulf of Thailand. 1-2.
- Muhammad Aw Yong Abdullah and B. S. Olsen, E. p. (1999). Tapis-New Opportunities from a Maturing Field. *SPE 54339* .
- S. Pisutha-Arnond & A. Sirimongkolkitti, V. P.-A. (2008). Carbon isotopic signature of CO2 in Arthit gas field, Northern Malay basin,the Gulf of Thailand.
- Scott W. Imbus L\*, B. J. (1998). Predicting Co2 occurence on a regional scale. 325,327,342,343,344.
- William C. Lyons, G. J. (2005). Enhanced Oil Recovery Method. In *Standard handbook of petroleum and natural gas engineering* (pp. 218-219). British Library Cataloguing in Publication Data.
- Y Samsudin, N. D. (2005). Enhanced Oil Recovey in Malaysia: Making It a Reality (Part 2). *SPE 95931* , 1,2,3.
- Zahidah Md. Zain, N. I. (2001). Evaluation of CO2 Gas Injection For Major Oil Production Fields in Malaysia –Experimental Approach Case Study: Dulang Field. *SPE 72106* .

## APPENDIX

### Gantt chart for FYP 1

The Gantt chart is a guideline for this project timeline. It can be changed from time to time depending on certain circumstances.

No.	Activities /Week	1	2	3	4	5	6	7	8	9	10	11	12	13
1	Selection of Project Topic	■	■											
2	Research done		■	■	■	■	■							
3	Proposal Submission				■									
4	Preliminary Report Submission					■								
5	Data gathering					■	■							
6	Literature Review						■	■	■	■				
7	Seminar					■								
8	Analysis of Carbon Dioxide data							■	■	■				
9	Submission of Progress Report								■					
10	Study on Genetic relation of produced CO <sub>2</sub>								■	■				
11	Study on commercialize mode of produced CO <sub>2</sub>									■	■	■	■	
12	Result Gathering						■	■	■	■	■	■	■	■
13	Submission of Interim Report													■
14	Oral Presentation													■

**Gantt chart for FYP 2**

No.	Activities /Week	1	2	3	4	5	6	7	8	9	10	11	12	13
1	Literature review	■	■											
2	Inas Field data analysis		■	■	■	■	■							
3	Learning Petroleum Experts Software		■	■	■	■	■							
4	Modelling EOR in Inas field by using MBal				■	■	■	■	■	■	■			
5	Analysis of results from modelling							■	■	■	■			
6	Submission of Progress Report								■					
7	Study on CO <sub>2</sub> flooding program.								■	■				
8	Modeling producer and injector well using PROSPER									■	■	■	■	
9	Result Gathering						■	■	■	■	■	■	■	■
10	Submission of Interim Report													■
11	Oral Presentation													

### Project Activities for FYP 1

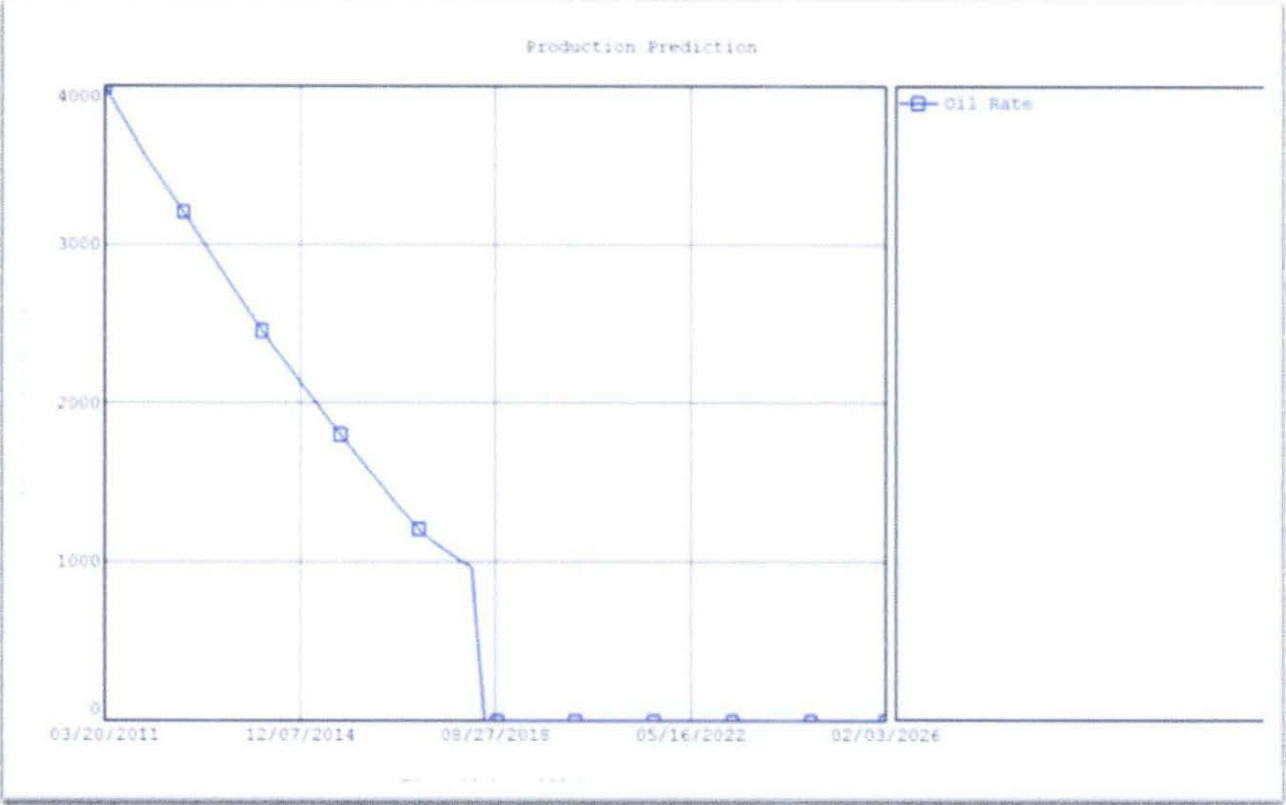
No	Action Item	Action By	Date	No
1	Selection of FYP topic	Students/ Supervisors	5/8/2010	Week 1
2	Prelim Research Work	Students	19/8/2010	Week 3
3	Submit Prelim Report	Students/Supervisors/ Coordinator	1/9/2010	Week 4
4	Project Work (Literature Review)	Students	8/9/2010	Week 5
5	Submit Progress Report	Students/ Supervisors/ Coordinator	17/9/2010	Week 8
6	Submit Interim Report	Students/ Supervisors Coordinator	20/10/2010	Week 10
7	Oral Presentation	Student/Supervisor		Week 14

### Project activities for FYP 2

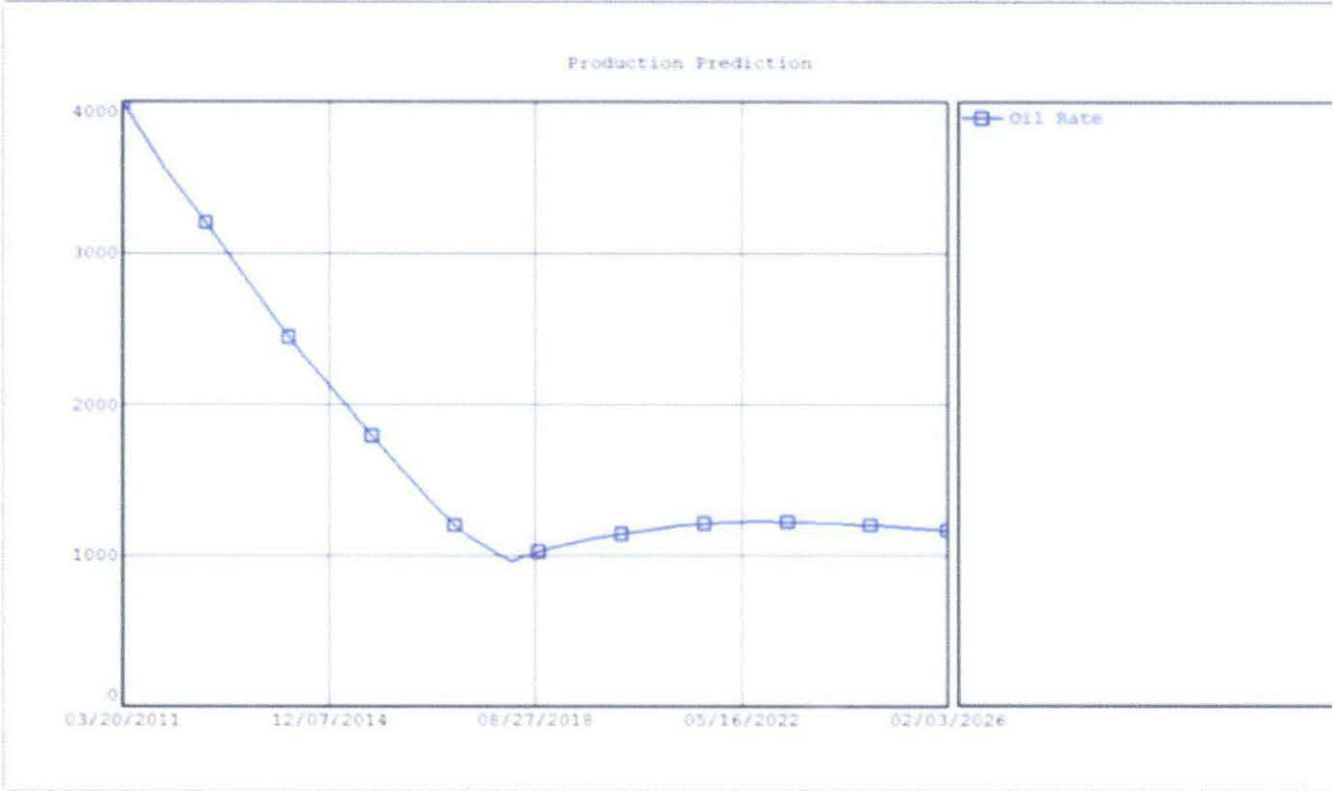
No	Action Item	Action By	Date	Note
1	Briefing & update on students progress	Coordinator / Students / Supervisors	8 February 2011	Week 3
2	Project work commences	Students		Week 1 -8
3.	Submission of Progress Report	Students	16 March 2011	Week 8
4.	PRE-EDX combined with seminar/ Poster Exhibition/ Submission of Final Report (CD Softcopy & Softbound)	Students / Supervisor / Internal Examiner / Coordinator	4 April 2011	Week 11

5.	EDX	Supervisors / FYP Committee	11 April 2011	Week 12
6.	Final Oral Presentation	Students / Supervisors	20 April 2011	Week 13
7.	Delivery of Final Report to External Examiner / Marking by External Examiner	FYP Committee / Coordinator	20-27 April 2011	Week 14
8.	Submission of hardbound copies	Students	04 May 2011	Week 16

Production vs. time plot (without CO<sub>2</sub> flooding)



Production vs. time plot (with CO<sub>2</sub> flooding)



# Reservoir modeling

## 1. Reservoir definition

**System Options**

Done  Cancel  Help

Tool Options	User Information
Reservoir Fluid: <input type="text" value="Oil"/>	Company: <input type="text"/>
Tank Model: <input type="text" value="Single Tank"/>	Field: <input type="text"/>
PVT Model: <input type="text" value="Simple PVT"/>	Location: <input type="text"/>
Production History: <input type="text" value="By Tank"/>	Platform: <input type="text"/>
Compositional Model: <input type="text" value="None"/>	Analyst: <input type="text"/>
<input type="button" value="EOS Model Setup..."/>	Reference Time: <input type="text" value="01/01/1900"/> date m/d/y

User Comments: \_\_\_\_\_ Date Stamp: \_\_\_\_\_ (Ctrl+Enter for new line)

## 2. Fluid properties input

**Oil - Black Oil: Data Input**

Done  Cancel  Help

Input Parameters		Separator
Formation GOR	<input type="text" value="336"/> scf/STB	<input type="text" value="Single-Stage"/>
Oil gravity	<input type="text" value="33"/> API	
Gas gravity	<input type="text" value="0.65"/> sp. gravity	
Water salinity	<input type="text" value="30000"/> ppm	
Mole percent H2S	<input type="text" value="0"/> percent	
Mole percent CO2	<input type="text" value="0"/> percent	
Mole percent N2	<input type="text" value="0"/> percent	

Correlations

Use Tables

Controlled Miscibility

### 3. PVT data matching

#### 3. Black oil correlation

Oil - Black Oil: Correlations - Oil

Done
  Cancel
  ? Help
  Hand Reset
  Plot

Pb,Rs,Bo
  Uo,Ug,Bg

Bubble Point	Glaso	Standing	Lasater	Vazquez-Beggs	Petrosky	Al-Marhoun
Parameter 1	0.869406	0.970285	0.965347	0.887605	0.886953	0.865273
Parameter 2	-374.027	-66.8497	-78.7849	-306.792	-309.09	-390.232
Std Dev.	9.3678e-11	1.68257e-11	2.00089e-11	7.68523e-11	7.68523e-11	9.73159e-11

Solution GOR	Glaso	Standing	Lasater	Vazquez-Beggs	Petrosky	Al-Marhoun
Parameter 1	1.36154	0.970303	0.977532	1.21722	1.48116	1.32741
Parameter 2	16.0857	33.2235	26.8708	26.6359	-39.3682	48.8391
Std Dev.	9.46827	11.198	6.15856	8.27437	13.6609	16.3432

Oil FVF	Glaso	Standing	Lasater	Vazquez-Beggs	Petrosky	Al-Marhoun
Parameter 1	3.65971	3.36631	3.40878	3.48434	3.55582	3.45989
Parameter 2	-3.03105	-2.7988	-2.84871	-3.01224	-2.97438	-2.90628
Parameter 3	0.491791	0.48716	0.534574	0.621353	1.47448	0.46724
Parameter 4	4.48741	4.50961	4.28241	3.86702	-2.23016	4.60512
Std Dev.	0.288611	0.287981	0.285456	0.285705	0.286825	0.287823

### 4. Reservoir properties input

Tank Input Data - Tank Parameters

Done
  Cancel
  ? Help
  Import

Tank Parameters	Water Influx	Rock Compress.	Rock Compaction	Pore Volume vs Depth	Relative Permeability	Production History
Tank Type	Oil					
Name	GM01					
Temperature	155	deg F				
Initial Pressure	2136.3	psig				
Porosity	0.25	fraction				
Connate Water Saturation	0.206	fraction				
Water Compressibility	3.22e-6	1/psi				
Initial Gas Cap	0.2					
Original Oil In Place	72.135	MMSTB				
Start of Production	03/20/2011	date m/d/y				
						<input type="checkbox"/> Monitor Contacts <input type="checkbox"/> Gas Coning <input type="checkbox"/> Water Coning
						Calculate Pb...

## 5. Prediction Calculation Setup

**Prediction Calculation Setup**

Done
  Cancel
  Help

Predict **Production Profile Using Well Models**

With **Profile from Production Schedule (No Wells)**

Water Injection
  Use Relative Permeabilities

Gas Injection

SWAG

Gas Lift Injection

Gas Recycling

Water Recycling

Voidage Replacement with water

Voidage Replacement with gas

Gas Cap Production

Aquifer Production

Prediction Step Size

Automatic (recommended)

User Defined  days

Prediction Start

Start of Production

End of Production History

User Defined  date m/d/y

Prediction End

Automatic

End of Production History

User Defined  date m/d/y

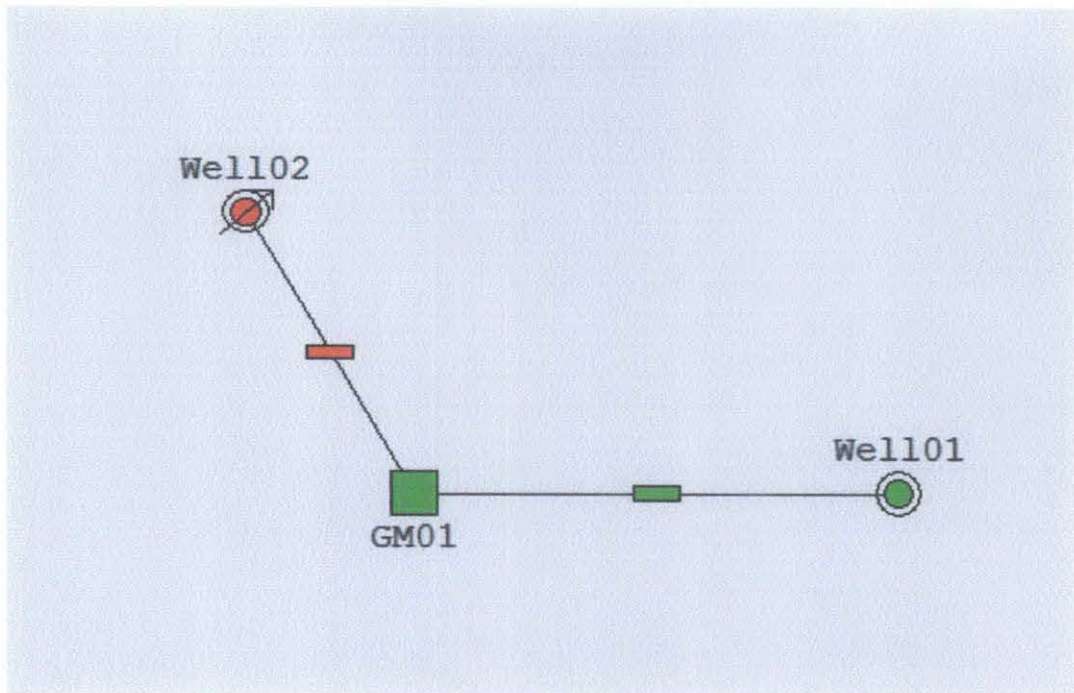
## 6. Production limitation and constrain

**Prediction Production and Constraints**

Done
  Cancel
  Help
  Plot
  Report
  Reset
  Import
  Layout
  Copy

Time	Step	Step	Step	Step	Step	Step	Step	Step	Step	Step	Step	Step	Step	Step	Step	Step
date m/d/y	Man Pres	Min Oil Rate	Max Oil Rate	Max Water Rate	Max Liquid Rate	Max Gas Rate	Gas Void Floplac.	Water Void Replac.	Gas Inj Man Pres	Min Inj Gas Rate	Max Inj Gas Rate	Mole % H2S	Mole % CO2	Mole % N2	Wat Inj Man Pres	
	psig	STB/day	STB/day	STB/day	STB/day	MMscf/day	percent	percent	psig	MMscf/day	MMscf/day				psig	
1	02/20/2011	100	100	200	300				100	5	6					
2																
3																
4																
5																
6																
7																
8																
9																

## 7. Well configuration



## 8. Well Schedule

**Well Schedule**

Done
  Cancel
  Help
  Reset

	Start Time	End Time	Number of Wells	Well Type Definition	Down Time Factor
	date m/d/y	date m/d/y			percent
1	03/20/2011	03/20/2040	1	Well01	
2	03/20/2018	03/20/2040	1	Well02	
3					
4					
5					
6					
7					
8					
9					
10					
11					
12					

Prediction from 03/20/2011 to 02/03/2026 date m/d/y

## 1. Well definition

System Summary (PRODUCER WELLOUT)

Done	Cancel	Report	Export	Help	Datestamp
------	--------	--------	--------	------	-----------

Fluid Description		Calculation Type	
Fluid	Oil and Water	Predict	Pressure and Temperature (offshore)
Method	Black Oil	Model	Rough Approximation
Separator	Single-Stage Separator	Range	Full System
Emulsions	No	Output	Show calculating data
Hydrates	Disable Warning		
Water Viscosity	Use Default Correlation		
Viscosity Model	Newtonian Fluid		

Well		Well Completion	
Flow Type	Tubing Flow	Type	Cased Hole
Well Type	Producer	Gravel Pack	No

Artificial Lift		Reservoir	
Method	None	Inflow Type	Single Branch
		Gas Coning	No

User information		Comments (Ctrl-Enter for new line)	
Company			
Field			
Location			

## 2. PVT input data

PVT - INPUT DATA (FDP GEMALA MERAHOUT) (Oil - Black Oil matched)

Done	Cancel	Tables	Match Data	Regression	Correlations	Calculate	Save	Open	Composition	Help
------	--------	--------	------------	------------	--------------	-----------	------	------	-------------	------

<input type="checkbox"/> Use Tables			
-------------------------------------	--	--	--

Input Parameters				Correlations	
Solution GOR	267	scf/STB		Pb. Rs. Bo	Glaser
Oil Gravity	33	API		Oil Viscosity	Beal et al
Gas Gravity	0.65	sp. gravity			
Water Salinity	30000	ppm			

Impurities		
Mole Percent H2S	0	percent
Mole Percent CO2	0	percent
Mole Percent N2	0	percent

### 3. PVT Correlations

PVT - Correlation Parameters (FDP GEMALA MERAH.OUT) (Oil - Black Oil matched)

Done	Cancel	Main	Export	Report	Reset All	Help
<b>Bubble Point</b>						
	Glaso	Standing	Lasater	Vazquez-Beggs	Petrosky et al	Al-Marhoun
Parameter 1	0.92593	1.04318	1.0653	0.95507	0.95316	0.90953
Parameter 2	-173.994	79.4118	115.366	-98.7741	-103.378	-221.106
Std deviation						
	Reset	Reset	Reset	Reset	Reset	Reset
<b>Solution GOR</b>						
	Glaso	Standing	Lasater	Vazquez-Beggs	Petrosky et al	Al-Marhoun
Parameter 1	1.55323	1.15388	1.1036	1.4022	1.9556	1.67113
Parameter 2	-9.4347	-3.80706	-4.7611e-13	-1.86398	-111.492	-1.87037
Std deviation						
	Reset	Reset	Reset	Reset	Reset	Reset
<b>Oil FVF</b>						
	Glaso	Standing	Lasater	Vazquez-Beggs	Petrosky et al	Al-Marhoun
Parameter 1	1.18525	0.95352	0.95357	0.86032	1.34285	0.96513
Parameter 2	-0.1911	0.045208	0.045152	0.13667	-0.36141	0.03235
Parameter 3	1	1	1	1	1	1
Parameter 4	1e-8	1e-8	1e-8	1e-8	1e-8	1e-8
Std deviation						
	Reset	Reset	Reset	Reset	Reset	Reset
<b>Oil Viscosity</b>						
	Beal et al	Beggs et al	Petrosky et al	Eqboqah et al		
Parameter 1	0.67564	0.81863	0.73223	0.56301		
Parameter 2	-1.23287	-0.38043	-0.77051	-4.51505		
Std deviation						
	Reset	Reset	Reset	Reset		

## 4. Inflow performance prediction

**Inflow Performance Relation (IPR) - Select Model**

Done Validate Calculate Report Transfer Data  
 Cancel Reset Plot Export  
 Help Test Data Sensitivity

Select Model  
Input Data

**Model and Global Variable Selection**

**Reservoir Model**

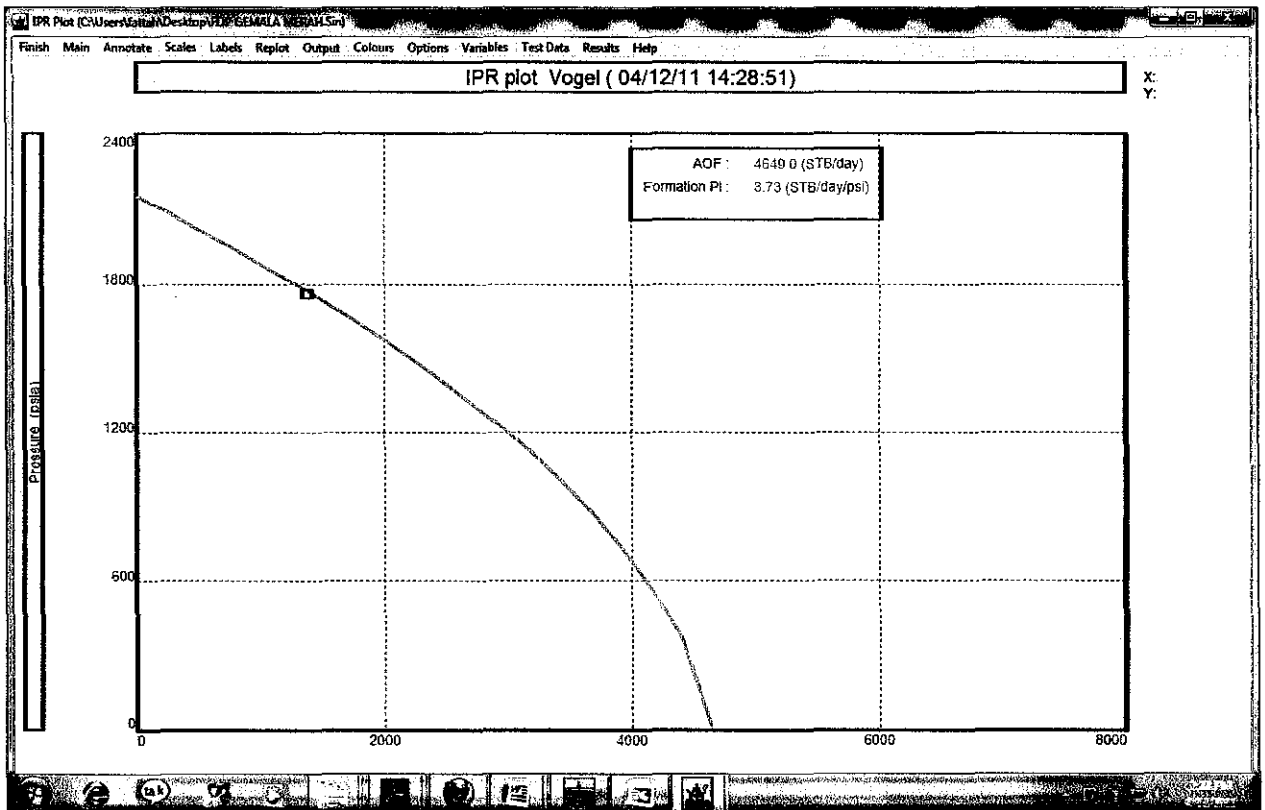
- PI Entry
- Vogel**
- Composite
- Darcy
- Fetkovich
- MultiRate Fetkovich
- Jones
- MultiRate Jones
- Transient
- Hydraulically Fractured Well
- Horizontal Well - No Flow Boundaries
- Horizontal Well - Constant Pressure Upper Boundary
- MultiLayer Reservoir
- External Entry
- Horizontal Well - dP Friction Loss In WellBore
- MultiLayer - dP Loss In WellBore
- SkinAide (ELF)
- Dual Porosity
- Horizontal Well - Transverse Vertical Fractures

**Mechanical / Geometrical Skin**

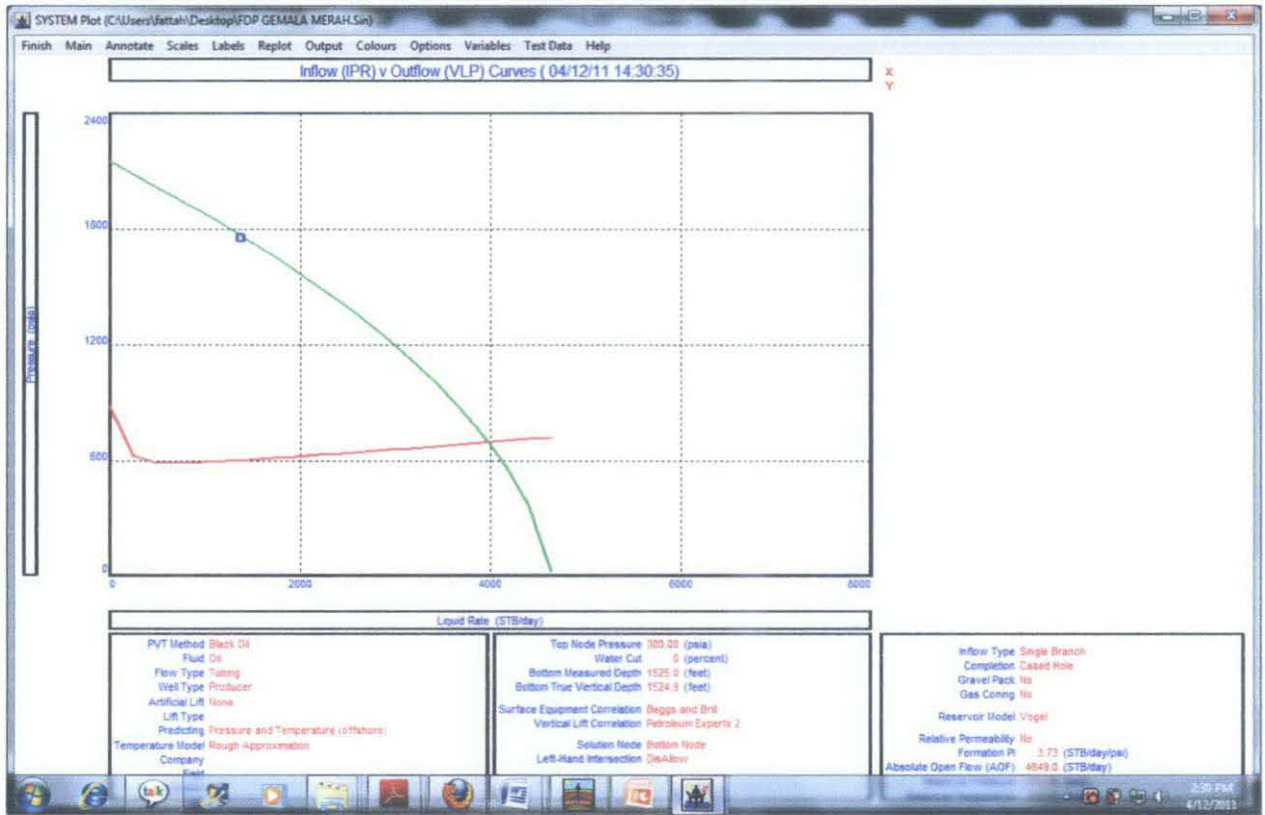
**Deviation and Partial Penetration Skin**

Reservoir Pressure	2151	psia
Reservoir Temperature	155	deg F
Water Cut	0	percent
Total GOR	267	scf/STB
Compaction Permeability Reduction Model	No	
Relative Permeability	No	

## 5. IPR plot



## 6. Inflow vs. outflow plot.



## Well injector performance

